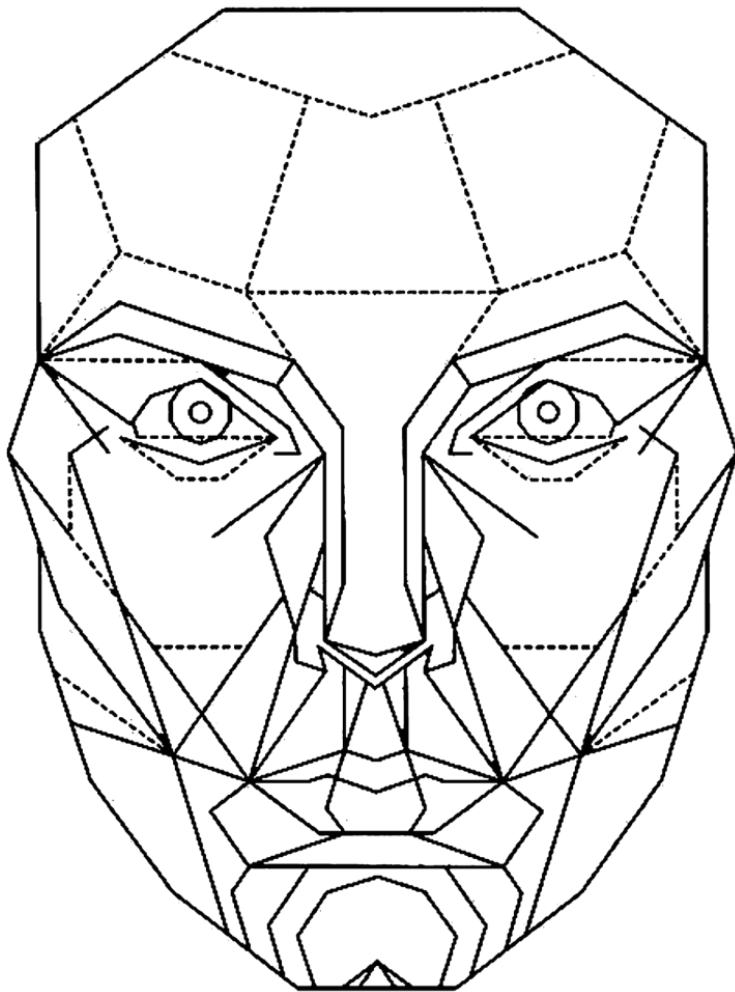


# MASTER THESIS

## 3D Technology in Manufacturing Pressure Masks for the Treatment of Hypertrophic Scarring following Oncological Facial Reconstruction

BSc. M.D. van Gaalen

Technical Medicine | Track Imaging & Intervention | January – August 2020



**Universiteit  
Leiden**  
The Netherlands



Delft  
University of  
Technology

**Erasmus  
University  
Rotterdam**



Master Thesis Technical Medicine

# “3D Technology in Manufacturing Pressure Masks for the Treatment of Hypertrophic Scarring following Oncological Facial Reconstruction”

by

M.D. van Gaalen

To obtain the degree of Master of Science  
at the Delft University of Technology,  
to be defended publicly on Tuesday 1<sup>st</sup> of September at 14.30.

## General information

Master program (track)	Technical Medicine (Imaging & Intervention)
Project duration	January 2020 – August 2020
Student number	4395565

## Graduation Committee:

Prof. dr. ir. J. Harlaar <sup>a</sup> ,	Chairman
Prof. dr. ir. R.H.M. Goossens <sup>b</sup>	Technical supervisor
Dr. E.M.L. Corten <sup>c</sup>	Medical supervisor
Dr. M. Wakkee <sup>d</sup>	External member
Dr. D. Dodou <sup>a</sup>	External member

<sup>a</sup> Department of Biomechanical Engineering, Delft University of Technology, Delft, the Netherlands

<sup>b</sup> Department of Industrial Design, Delft University of Technology, Delft, the Netherlands

<sup>c</sup> Department of Plastic, Reconstructive and Hand Surgery, Erasmus University Medical Center, Rotterdam, the Netherlands

<sup>d</sup> Department of Dermatology, Erasmus University Medical Center, Rotterdam, the Netherlands

*An electronic version of this thesis is available at <https://repository.tudelft.nl>*

# Preface

This year started with a great adventure: I went to Masanga, Sierra Leone, to continue setting up a 3D lab in the Masanga hospital. My bags were filled with filaments and a hand-held 3D scanner. Together with the local physiotherapist and under the guidance of a great support team in the Netherlands, we succeeded to fabricate several 3D printed prostheses, splints and other medical aids for amputees. This project was without a doubt one of most beautiful experiences during my education. I would like to express my gratitude to Jaap Harlaar and Lars Brouwers for giving me the opportunity to go abroad.

By working with 3D scanning and 3D printing techniques, my enthusiasm for the applications of these technologies became stimulated. As a result, this graduation project was created. This project could not have taken place without the supervision and help of many people.

First of all, I would like to thank Richard Goossens and Eveline Corten for being my supervisors during this project. Your endless enthusiasm and support kept me going during these challenging times originating from the COVID-19 pandemic.

Richard, I wish you great success with your role as Program Director of the Convergence Health and Technology, a collaboration that makes me, as a Technical Physician (in training), very enthusiastic. I feel honoured that, despite your busy schedule, you have been willing to guide me during this project. I hope our paths will cross again in the future!

Eveline, without you, there could have been no graduation project at all. I will never forget our first meeting; You showed me your mind map full of plans for future research at the Department of Plastic and Reconstructive Surgery, ranging from the application of 3D scanning and 3D printing to the use of virtual and augmented reality. Your enthusiasm is contagious! I really appreciate your constructive feedback and how you guided me in the right direction at any time. I wish you every success with all your future (research) plans!

Several other people were involved during this project. First, I would like to thank Carlo Colla and his colleagues in the MUMC+. Thank you for sharing your knowledge and inspiring us for undertaking this project!

Also, I would like to thank Bertus Naagen (Bodylab, Industrial Design), Geert Springeling (Department of Experimental Instrumentation, Erasmus MC), Don van Eeden and Roland van der Velden (Model Making and Machine Lab) for making use of the 3D scanners, 3D printers and other facilities. I would like to thank Joan Saridin (Anaplastologist, Erasmus MC) for introducing me to the wonderful world of silicone facial prosthetics.

Further, I would like to thank Marlies Wakkee and Dimitra Dodou for being part of my graduation committee!

Last but certainly not least, I would like to thank my family, family in law and friends for their endless love and encouragement. Especially thanks to Mitchel for always being there, even in this report!

*M.D. van Gaalen*

*18/08/2020, Delft*

# Summary

## Introduction

Transparent facial pressure masks with silicone sheeting are used as a non-invasive treatment option for hypertrophic scarring following oncological facial reconstruction. These masks are fabricated using conventional plaster moulds, which is labour-intensive and requires an experienced orthotist or prosthetist. 3D scanning and 3D printing are promising technologies that could replace the current traditional fabrication process. The aim of this thesis is to evaluate whether 3D technology is suitable to replace the traditional fabrication method of transparent facial pressure masks; and is able to produce a mask that provides adequate pressure therapy.

## Methods

First, a systematic review was performed to identify suitable 3D scanning and 3D printing techniques for fabrication of the facial mask and to find pressure assessment tools.

Subsequently, 3D scanners, 3D printers, software and pressure assessment tools were analyzed for technical feasibility and availability.

Based on this analysis, a pilot study was performed in which the most optimal workflow to fabricate facial pressure masks using 3D technology was designed. The most optimal workflow was identified in terms of (1) workload (man-hours, degree of automation and need for human expertise); (2) patient comfort; (3) total time; and (4) costs;

Two masks were fabricated for a healthy volunteer using two different moulds: a 3D printed mould and a conventional plaster mould. These masks were compared in terms of comfort and blanching of the skin as indirect measures for pressure distribution.

## Results

A hand-held structured light 3D scanner (Artec Eva, Artec 3D), easy-to-use CAD software (Meshmixer, Autodesk, Inc.) and Fused Deposition Modeling (Ultimaker 2+, Ultimaker) appear to be the most suitable tools for the fabrication of a facial mask. As pressure distribution cannot be assessed directly yet, due to the lack of reliable sensors, the most suitable tools to assess pressure distribution indirectly are patient comfort and blanching of the skin.

The most optimal workflow to fabricate a facial mask using 3D printing techniques consists of 3D scanning and 3D printing of a positive mould followed by vacuum forming of Silon-STs® over the positive mould. This is a partly automated process that still needs human expertise. Based on an estimation of time and costs, the fabrication process is quicker and cheaper than the conventional method. Although the manipulation process during aftercare takes longer and is more expensive, the number of man-hours remains the same and patient comfort increases.

The facial mask fabricated using 3D scanning and printing techniques for the moulding process causes undesirable blanching of the skin at the nasal bridge and the healthy volunteer expressed discomfort due to this pressure point. The facial mask fabricated using a conventional plaster mould causes discomfort at the cheeks. Therefore, both masks will need design adjustments to provide adequate pressure therapy.

## Conclusion

Based on our preliminary results 3D technology seems suitable to partly replace the traditional fabrication method of transparent facial pressure masks. To further optimize and validate the proposed workflow, future research should focus on digital mould modification and more objective pressure measurement tools. Future goals in a clinical setting will be to evaluate (1) cost-effectiveness; (2) long-term clinical effects in patients and (3) patient reported outcome measures.

# List of abbreviations

CAD	Computer-aided-design
LDI	Laser Doppler Imaging
FEM	Finite Element Modeling
STL	Stereolithography
FDM	Fused Deposition Modeling
SLA	Stereolithography Apparatus
SLS	Selective Laser Sintering
VAS	Visual Analogue Scale
PLA	Polylactic acid
ABS	Acrylonitrile butadiene styrene
PETG	Polyethylene terephthalate glycol
PC	Polycarbonate
CNC	Computer Numerical Control

# Table of contents

Preface .....	2
Summary .....	3
List of abbreviations .....	4
Table of contents.....	5
1 Introduction.....	7
1.1 Clinical context .....	7
1.2 Research purposes .....	7
1.3 Thesis outline .....	8
2 Theoretical framework .....	9
2.1 (Patho)physiology of hypertrophic scarring .....	9
2.2 Epidemiology and etiology of (facial) hypertrophic scarring .....	9
2.3 Facial hypertrophic scarring and its impact.....	9
2.4 Scar prevention and treatments.....	10
2.4.1 Pressure therapy .....	10
2.4.2 Silicone therapy.....	10
2.4.3 Invasive treatment .....	11
2.5 Transparent facial pressure masks - current fabrication method .....	11
2.5.1 Fabrication of the negative mould .....	11
2.5.2 Fabrication of the positive mould.....	11
2.5.3 Production of the facial mask – Silicone inner lining .....	13
2.5.4 Production of the facial mask – Rigid part.....	13
2.5.5 Fitting and delivery .....	13
3 Systematic review.....	14
3.1 3D technology .....	14
3.1.1 3D scanning technology .....	14
3.1.2 Computer Aided Design (CAD) .....	15
3.1.3 3D printing technology.....	15
3.2 Facial pressure (distribution) assessment tools.....	17
3.2.1 Pressure sensors.....	17
3.2.2 Laser Doppler Imaging.....	18
3.2.3 Comfort .....	18

3.2.4	Digital imaging.....	18
3.2.5	Finite element model .....	18
3.2.6	3D scanning techniques.....	18
4	Pilot study.....	19
4.1	Methods and Materials .....	19
4.1.1	Design optimal workflow and prototype .....	19
4.1.2	Validation .....	19
4.2	Results .....	20
4.2.1	Design optimal workflow and prototype .....	20
4.2.2	Validation .....	32
5	Discussion .....	35
6	Conclusion .....	37
	Appendices.....	41
	Appendix I Design requirements .....	41
	Appendix II Workflows .....	43
	Appendix III Literature review .....	54

# 1 Introduction

## 1.1 Clinical context

Hypertrophic scarring following oncological facial reconstruction is a complex problem, causing both physical and psychological complaints [1, 2]. Hypertrophic scars are elevated scars caused by an abundant deposition of collagen at the location of injury [3].

Pressure therapy is the norm in non-invasive treatment of hypertrophic scars. It has been shown that exerting mechanical pressure can lead to reduced scar thickness and scar erythema [4]. Several other non-invasive interventions are available to both prevent and treat excessive scar formation [5]. In addition to pressure therapy, silicones have become a first-line non-invasive treatment of hypertrophic scars. Silicone therapy shows positive effects on scar erythema and pliability [6]. Combined therapy consisting of both pressure and the use of silicones is suggested to be more effective than pressure or silicone therapy alone [7, 8]. Therefore, biocompatible transparent facial pressure masks with silicone sheetings were developed that are attached to the head by a harness system with straps and anchors [9-11].

Currently, the facial pressure masks with silicone sheeting are fabricated using conventional plaster moulds, which is labour-intensive and requires an experienced orthotist or prosthetist [12]. The MUMC+, Maastricht, is the only place in the Netherlands where such an orthotist is employed. Therefore, not every patient with hypertrophic scarring following oncological facial reconstruction who is eligible for treatment by a silicone facial pressure mask can be treated. As the number of patients with facial hypertrophic scarring is increasing due to the rising numbers of skin cancer, it is desirable that this treatment can be offered to more patients [13-15].

3D scanning and 3D printing are promising techniques that can potentially replace the current traditional fabrication process [16, 17]. However, Colla et al. hypothesized that a facial mask fabricated using 3D printing techniques results in a less optimal pressure distribution on the face when compared to the traditionally fabricated facial mask [12]. To test this hypothesis, we aim to evaluate whether 3D technology is suitable to replace the traditional fabrication method of transparent facial pressure masks, and is able to produce a mask that provides adequate pressure therapy.

## 1.2 Research purposes

The primary aim of this thesis is to evaluate whether 3D technology is suitable to replace the traditional fabrication method of transparent facial pressure masks, and is able to produce a mask that provides adequate pressure therapy.

Secondary aims are:

- 1) To design the most optimal workflow for the fabrication process of the facial masks using 3D scanning and 3D printing techniques and to fabricate a prototype according to this workflow.
- 2) To assess pressure distribution on the face while wearing a facial mask fabricated using 3D scanning and 3D printing techniques.

### **1.3 Thesis outline**

In order to reach the aims outlined in section 1.2, several steps were undertaken. The theoretical framework is presented in Chapter 2 of this thesis and provides the rationale for conducting this research. This thesis contains a systematic review and a pilot study. Chapter 3 contains the key findings of the systematic review. The results of the pilot study are presented in Chapter 4. Chapter 5 contains the general discussion, including recommendations for future research. A conclusion is presented in Chapter 6.

# 2 Theoretical framework

## 2.1 (Patho)physiology of hypertrophic scarring

Scar formation is a result of the wound healing process following physical injury. The wound healing process can be grouped into three overlapping phases: inflammation (4 to 6 days), cell proliferation (4 to 24 days), and matrix remodeling (21 days to 2 years) [18-20]. This mechanism is regulated by fibroblast activity, fibrin deposition, angiogenesis, and production of fibronectin and collagen. Synthesis and degradation of tissue are balanced to avoid excessive scar formation [3].

Some scars cause considerable problems as a result of abnormal wound healing. Excessive scar formation may develop after any insult to the deep dermis, including surgery and burn injury [21]. Hypertrophic scars are elevated scars caused by an abundant deposition of collagen at the location of injury [3]. Physical symptoms include pain, itching and scar contractures [22, 23].

Hypertrophic scars appear within 4 to 8 weeks following wound closure and progress for a period up to 6 months [24]. Over a period of a few years, some hypertrophic scars may regress spontaneously [25].

## 2.2 Epidemiology and etiology of (facial) hypertrophic scarring

Depending on the depth of the wound, the incidence rates of hypertrophic scarring vary from 40% to 70% following surgery and up to 91% following burn injury [26, 27]. Common risk factors are young age, inflammation and tension on the wound [28].

Major facial defects are mainly caused by the surgical removal of skin cancer, the most common type of cancer with increasing incidence, especially in people younger than 30. Facial skin cancer is common, due to the fact that the face is frequently exposed to ultraviolet (UV) radiation [29]. It results in high economic costs [13-15].

Mohs micrographic surgery is considered the most effective technique for treating facial skin cancer. This procedure provides precise removal of the lesion, while healthy tissue is spared [30]. Due to malignant growth, the resulting defect may be extensive. In that case, facial reconstruction by the plastic surgeon is needed and facial hypertrophic scarring can be the result [31].

## 2.3 Facial hypertrophic scarring and its impact

Facial hypertrophic scarring is a complex problem, causing both physical and psychological complaints [1, 2]. As the face is essential for social interaction, psychosocial effects of facial scarring include diminished social interaction with a disruption of daily activities as a result. This, in turn, creates vulnerability to developing mental health disorders. Patients are reporting higher levels of anxiety, depression and an overall lower quality of life [32].

## 2.4 Scar prevention and treatments

Currently, several scar management measures have been advocated to prevent and treat excessive scar formation:

### 2.4.1 Pressure therapy

Since the 1960s, pressure therapy is the norm in non-invasive treatment of hypertrophic scars. It has been shown that exerting mechanical pressure can lead to reduced scar thickness and scar erythema [4]. The effect could partly be explained by reduced oxygen tension through occlusion of small blood vessels. As a result, collagen synthesis and fibroblast proliferation decrease [33]. However, the exact mechanism of action is still poorly understood.

Pressure can be exerted on scars by means of garments, splints, casts or transparent facial masks (*Figure 1*). Recommendations for the amount of applied pressure and the duration of therapy are based on empirical observations. It is recommended to apply a continuous pressure of 15-40 mmHg (2-5,3 kPa) for more than 23 hours for at least six months [33]. Therefore, it is considered to be a demanding therapy, which challenges patient's compliance [34]

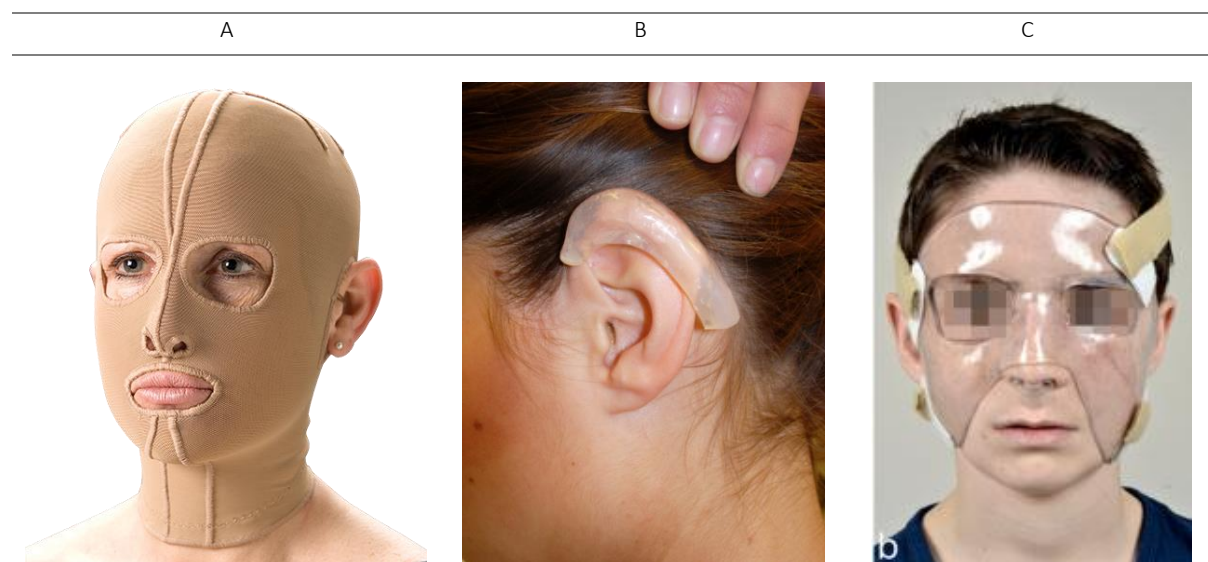


Figure 1 Different types of pressure therapy. Pressure is exerted by a) a pressure garment [35]; b) A pressure splint [36]; c) A transparent facial pressure mask [37].

### 2.4.2 Silicone therapy

Silicone therapy is believed to prevent and treat excessive scar formation through occlusion and subsequent tissue hydration [38]. The stratum corneum, the top layer of the skin, serves as a physiological barrier. In newly formed scar tissue, the stratum corneum is underdeveloped and dehydration is a problem. As a response to dehydration, fibroblasts produce more collagen to aid water retention [39]. Silicone gel sheetings simulate the occlusion properties of the stratum corneum [40, 41]. Therefore, the stratum corneum functions are normalized and excessive collagen production is suppressed [42].

Silicone sheetings are made of medical-grade silicone. The silicone sheetings should be worn for more than 12 hours a day for at least 2 months. For moving parts of the body, silicone gel is favoured. Silicone gel should be applied twice a day [39].

### 2.4.3 Invasive treatment

In patients with long-standing hypertrophic scars, more invasive treatment is indicated. Currently, the use of intralesional corticosteroids is the only invasive non-surgical therapy which has enough supporting evidence to be included in evidence-based guidelines [43]. Response rates vary from 50% to 100% and the recurrence rate is 9% to 50% [44]. Furthermore, non-compliance with the treatment can be caused by excessive pain during the corticosteroid injections. Other side effects are hypopigmentation, skin atrophy and telangiectasias [45]. Permanent (> one year) hypertrophic scars may be treated surgically [43]. In case of contractures with functional impairment, surgery is indicated to release tension in the scar [43]. However, optimal prevention and early non-invasive treatment is preferred to prevent surgery.

## 2.5 Transparent facial pressure masks - current fabrication method

Combined pressure and silicone therapy is suggested to be more effective than pressure or silicone therapy alone [7, 8]. Therefore, biocompatible transparent pressure masks with silicone sheetings can be fabricated to treat facial hypertrophic scarring.

Transparent masks allow observing blanching of the scars, the desired effect of applied pressure. Furthermore, a transparent mask provides a better cosmetic sight. The facial masks are attached to the head by a harness system with straps and anchors [11].

Currently, the facial pressure masks with silicone sheeting are fabricated using plaster moulds, which is labour-intensive and requires an experienced orthotist or prosthetist [12]. The current workflow for the production of facial pressure masks with silicone sheeting is described by Colla et al. [12] and is outlined in *Figure 2*.

### 2.5.1 Fabrication of the negative mould

First, a negative mould is created by covering the face with plaster strips. During hardening of the plaster, the orthotist manually manipulates and steers soft tissue parts to create a functional mask. The expected result of this manipulation is to increase pressure on facial areas where therapeutic pressure is desirable. It is hypothesized that this process results in superior pressure distribution of the mask on the face when compared to a silicone facial pressure mask fabricated using 3D printing techniques [12].

### 2.5.2 Fabrication of the positive mould

A positive mould is fabricated by filling the negative mould with liquid plaster. This positive mould contains all the contours and irregularities of the face. The orthotist corrects and reduces the thickness of the facial hypertrophic scars by smoothing the corresponding area on the positive plaster mould with a rasp and scrapers. This leads to increased pressure over the facial hypertrophic scars in the (final) rigid mask. As both the rigid and silicone part of the mask are fabricated using the positive plaster mould, the resulting facial mask will apply more pressure on these areas. After sanding the mould with a very fine grit, the mould is dried in an oven.

### ***Fabrication of negative mould***

1. Vaseline applied to the face
2. The scar marked on the face
3. Plaster strips applied on the face
4. Tissue steering during hardening
5. Location buckle anchors marked
6. Face cleaned from plaster residues

### ***Fabrication of positive mould***

1. Mix water and porous plaster
2. Remove air bubbles (vibration)
3. Fill negative mould with plaster
4. Hardening of plaster (20 min)
5. Smooth plaster mould to correct and reduce scar thickness
6. Mould dried in oven (2-3h)

### ***Production of the facial mask***

#### **Silicone lining:**

1. 2 components merged & rolled
2. Silicones applied to mould
3. Vacuum forming
4. Silicone liner in oven for 8h

#### **Rigid mask:**

1. Uvex polycarbonate in oven
2. When pliable, applied to mould
3. Vacuum forming
4. Trim and smooth edges
5. Buckle anchors attached
6. Silicone lining attached with Velcro straps through nickle loops

### ***Fitting and delivery***

1. Pressure visually checked by looking for blanching of scars.
2. Adjust tightness of bandages

#### **During therapy (+/- 7 times):**

Rigid mask heated with small blow dryer and placed on altered mould

1

50 min

2

4 hours

3

14 hours

4

1.5 hours



*Figure 2* The manual fabrication method described by Colla et al. The workflow consists of the fabrication of a negative mould; the fabrication of a positive mould; the production of the rigid facial mask with silicone inner lining and a fitting and delivery phase. During the aftercare phase, the facial masks are adjusted approximately seven times.

### 2.5.3 Production of the facial mask – Silicone inner lining

The silicone inner lining contains two components of medical silicones (Ottobock® HTV-silicones, 35 Shore). A Shore hardness 35A corresponds with the finding of Lewis et al. who showed that the flexibility of materials used in facial prostheses should range from 25 to 35 Shore A [46].

The two components are merged and rolled together. The result is a silicone inner lining with a thickness of 1 mm without air bubbles. The silicones are applied to the positive mould on a vacuum forming platform and air is removed. The silicone inner lining is placed in an oven until the silicones are vulcanized.

### 2.5.4 Production of the facial mask – Rigid part

A polycarbonate plate is heated in an oven. When the plate becomes pliable, it is applied to the positive plaster mould on a vacuum forming platform and air is removed.

A hand-held circular saw is used to trim the edges of the silicone liner and the rigid mask. Buckle anchors with nickel loops are attached to the rigid mask. Velcro straps that are attached to the silicone liner go through these loops. In this way, the silicone inner lining is fixated to the transparent rigid part and can be easily removed for cleaning purposes.

### 2.5.5 Fitting and delivery

In most cases, a 5-point harness is used to fit the mask onto the patient (Figure 3). Parry et al. described that a 5-point design results in the most optimal and even facial pressure distribution [11]. Pressure on the face is visually checked by looking for appropriate blanching of scars. Blanching is considered appropriate when scar tissue becomes slightly paler than healthy skin. The tightness of the bandages can be adjusted to apply more or less pressure on the face. During therapy, the rigid mask needs to be adjusted several times as the thickness of the scars decreases. The orthotist adjusts the positive plaster mould using scraping tools to remove plaster at the place where the thickness of the scar decreased. The rigid part is heated using a small blow dryer and placed on the adjusted positive mould.

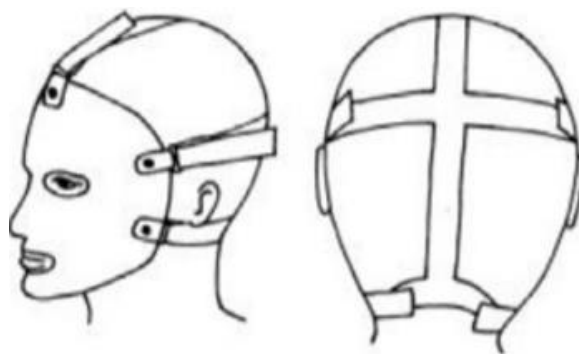


Figure 3 5-point harness design described by Parry et al.

# 3 Systematic review

A systematic review was performed to identify suitable (1) 3D scanning and 3D printing techniques for the fabrication of a facial mask and (2) pressure assessment tools. The literature review is presented in Appendix III.

3D scanners, 3D printers, CAD software and pressure assessment tools presented in the literature review were analysed for technical feasibility and availability. The key findings of the literature review and results of the analysis are presented in this chapter.

## 3.1 3D technology

### 3.1.1 3D scanning technology

3D scanning is a technique that can be used to capture the shape of the face using a static or hand-held 3D scanner. Non-contact 3D scanning techniques decrease patient discomfort and are less labour-intensive for the orthotist. Some 3D scanners can collect shape and colour data simultaneously. Several non-contact 3D scanning technologies exist, which rely on different physical principles outlined in *Table 1*.

Table 1 Short descriptions of non-contact 3D scanning technologies

3D scanning technique	Description
Laser-beam technology	A scanning technique that projects a laser beam onto the object and captures the reflected light. The surface shape is formed based on the time of flight of the laser beam. The time of flight increases with the distance between the sending device and the object.
Structured light 3D scanning	A scanning technique that projects light onto the object and captures the deformed light pattern by cameras.
Photogrammetry	A scanning technique based on (multiple) photographs.

Hand-held structured light 3D scanners (Creaform Go!Scan 50, Creaform 3D; and Artec Eva, Artec3D) and a static photogrammetry 3D scanner (3dMD face, 3dMD) are available for use during this project (*Figure 4*). The Creaform Go!Scan 50 is available at the Department of Oral and Maxillofacial Surgery, Erasmus MC. The Artec Eva is available at the Body Lab, Faculty of Industrial Design, TU Delft.

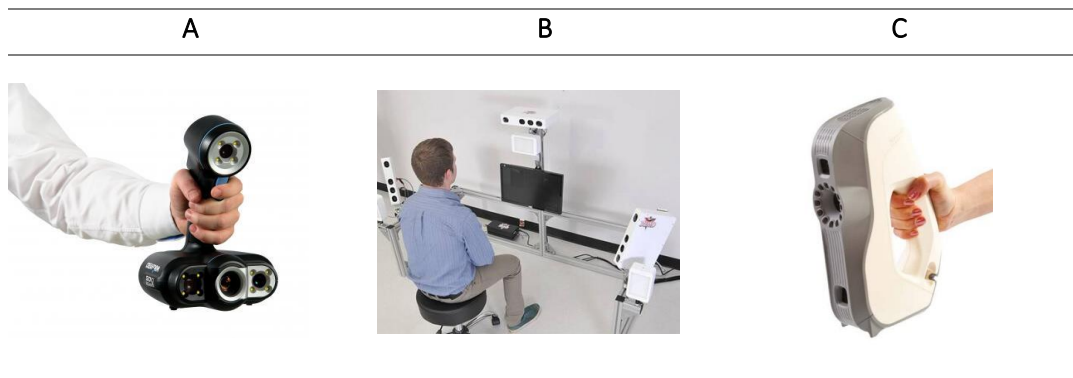


Figure 4 Available 3D scanners during this project; a) Creaform Go!Scan 50; b) 3dMD face; c) Artec Eva

### 3.1.2 Computer Aided Design (CAD)

Acquired 3D scans can be turned into 3D models, stereolithography (STL) files. The STL files can be imported in Computer Aided Design (CAD) software.

CAD software is used for creation, analysis and optimization of a (3D) design. By using CAD software, the design process becomes more efficient and the quality of a design could be improved [47]. When finalized, the digital object can be used as input for 3D printing [47]. Based on the results of the literature review, several software programs are suitable to design custom-made products. Most studies investigated the use of 3-Matic (Materialise) and Geomagic Studio (3D systems). However, easy-to-use free CAD software Meshmixer (Autodesk) seems to be a more feasible alternative while taking into account practical considerations such as technical feasibility and availability.

### 3.1.3 3D printing technology

3D printing, or additive manufacturing, is a process for making physical objects from a 3D digital model. An STL file is converted into a series of thin layers. Material is deposited and added together, typically layer by layer.

Most studies investigated the use of the 3D print technique Fused Deposition Modeling (FDM) with biocompatible polylactic acid (PLA) as 3D print material to print. Other suitable 3D printing techniques are stereolithography apparatus, selective laser sintering, material jetting and binder jetting. The description of the 3D printing techniques is presented in *Table 2*. No studies showed the possibility to 3D print medical-grade silicones directly.

Table 2 Short descriptions of 3D printing techniques

Technique	Description
Fused deposition modeling (FDM)	Layer-by-layer deposition of a thermoplastic filament by a moving heated extruder head (nozzle).
Stereolithography apparatus (SLA)	Light-sensitive resins (liquid materials) are turned into solid 3D objects by shining an ultraviolet laser on it.
Selective Laser Sintering (SLS)	A high power laser is used to fuse small particles of metal, plastic, ceramic or glass powder.
Material Jetting	Deposition of droplets of a photosensitive material on a building platform. After each layer, UV light activates the curing process.
Binder jetting	A liquid binder agent is deposited onto a powder bed, bonding the powder together to form a solid part.

Fused Deposition Modeling (Ultimaker 2+, Ultimaker; and DDDrop Twin Leader, DDDrop 3D printers) and Material Jetting (Objet 30 Pro, Stratasys) are available for use during this project (*Figure 5*). All 3D printers are situated at the Department of Experimental Instrumentation, Erasmus MC. Due to COVID-19 restrictions, 3D printers at the Applied Labs, Faculty of Industrial Design, were not available for use.

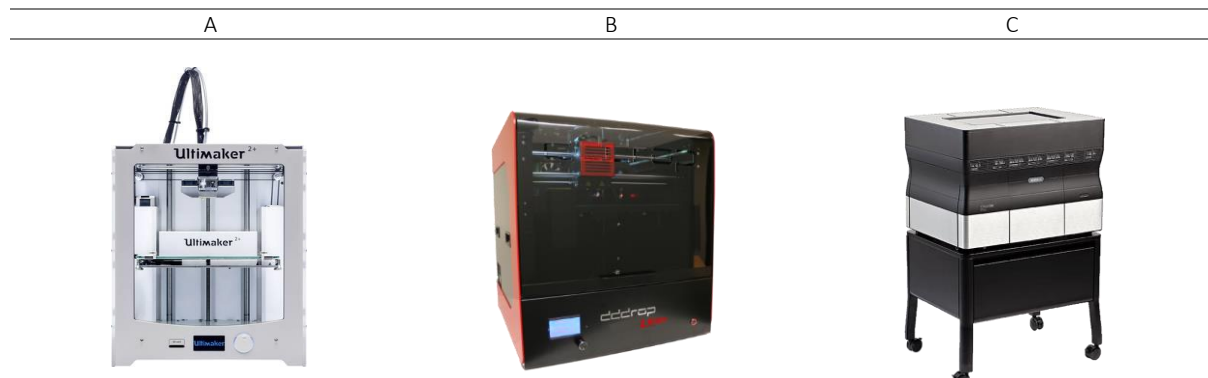


Figure 5 Available 3D printers during this project; a) Ultimaker 2+; b) DDDrop Twin Leader; c) Objet 30 Pro, Stratasys

## Subtractive manufacturing and vacuum forming

As 3D printing is an additive manufacturing technique, subtractive manufacturing techniques fell outside the scope of the literature review. In subtractive manufacturing, material is cut away to create a finished part. Cutters are used to shape the piece. In contrast, additive manufacturing involves parts being created layer-by-layer with little waste [48] (*Figure 6*). Rogers et al. successfully investigated a fabrication process using 3D scanning, milling and vacuum forming [49]. This process could be an appropriate alternative to 3D printing and should be further investigated.

Both foam milling and vacuum forming facilities are available at the Model Making and Machine Lab, Faculty of Industrial Design, TU Delft.

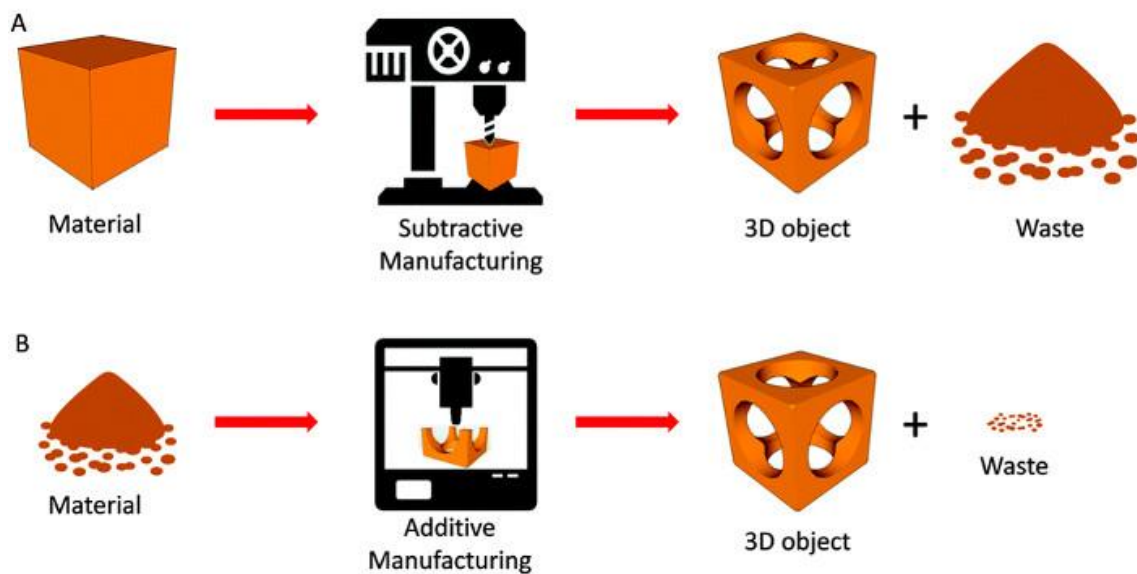


Figure 6 Subtractive versus additive manufacturing: In subtractive manufacturing, material is cut away to create a finished part. Cutters are used to shape the piece. Additive manufacturing involves parts being created layer-by-layer.

## 3.2 Facial pressure (distribution) assessment tools

The literature review provides an overview of facial pressure (distribution) assessment tools. In theory, all tools mentioned in the literature review are complementary to each other in the evaluation of the (indirect) effects of the applied pressure. Practical considerations such as technical feasibility and availability should be taken into account while identifying the most optimal tools for use during this project.

### 3.2.1 Pressure sensors

As it is preferable to measure the applied pressures directly, several thin pressure sensors were evaluated. Based on the results of the literature review, the Pliance X [16], Flexiforce [50] and Tekscan-I-Scan [51] seem appropriate pressure sensors. However, Flexiforce and Tekscan-I-Scan sensors are reportedly temperature sensitive, less accurate at lower levels of pressure and extensive calibration is needed prior to use. The PlianceX system is not validated for use on skin surfaces with high concavity, such as the face [52]. Furthermore, the pressure monitoring devices have not been tested during dynamic movements [52].

An alternative to pressure sensors is the use of pressure measurement film (Prescale, Fujifilm). This film (200  $\mu\text{m}$ ) can be placed between two objects and the amount of pressure can be visualized by color density. Red patches appear on the film where pressure is applied. The color density varies according to the pressure levels. A disadvantage of pressure measurement film is that it is not able to reliably measure pressures below 375 mmHg (50 kPa). Therefore, pressure measurement film is not suitable for this project.

Due to the fact that there are no reliable sensors to measure the interface pressure between a facial mask and the face yet, other alternatives were investigated to assess facial pressure distribution.

### **3.2.2 Laser Doppler Imaging**

Blanching of the skin or scar due to pressure correlates with a decreased blood flow. Allely et al. showed that Laser Doppler Imaging (LDI) can be used to measure perfusion at high percent pixel validity through a transparent facial mask [53]. A decrease in measured perfusion units was observed during pressure application. This finding implied that LDI can be used to objectively determine the efficacy of pressure by evaluating perfusion in hypertrophic scars [53].

A combination of 3D scanning techniques and an LDI perfusion scan could be valuable in the development of facial pressure masks by computerized manufacturing. However, LDI is an expensive technique that is not widely used. The initial investment of equipment is €57.590 and investments during use and maintenance must be added to this amount. The mean price of an LDI scan per patient is €151 [54]. This technique does not seem to be cost-effective if only used for this purpose.

### **3.2.3 Comfort**

Improper fit of the facial mask can cause patient discomfort and pressure ulcers. Evaluating the comfort level can be useful to assess facial pressure distribution. A rating scale frequently used is the 10-cm Visual Analogue Scale (VAS), an instrument used to measure the intensity of symptoms [55, 56]. The scale ranges from 0 to 10, where 0 represents no discomfort and 10 extreme discomfort. Comfort levels can be rated at the forehead, nasal bridge, chin and cheeks.

### **3.2.4 Digital imaging**

Blanching of the skin or scar due to pressure can be captured by digital cameras. Yamamoto et al. described the use of ordinary digital cameras and ImageJ freeware to quantify erythema and pigmentation for the analysis of skin tests and the management of skin diseases [55]. However, the results are highly dependent on the specifications of the camera used and the circumstantial conditions, such as illumination and distance from the objects. Several studies described that visually checking for blanching is an appropriate method to assess facial pressure distribution as well [12, 16, 57, 58].

### **3.2.5 Finite element model**

A finite element model is a computational technique that can be used to simulate and assess the biomechanics of the musculoskeletal system, including soft tissue mechanics. A finite element model of the head can be created to simulate and predict the mechanical response to application of the facial mask [17, 59]. The result could be used to design a facial mask that provide an even facial pressure distribution. However, detailed information of intracranial components and soft tissues derived from CT or MR scans is needed to create a high-quality human headform. However, most patients with hypertrophic facial scars due to facial reconstruction do not routinely undergo a CT or MR scan. Therefore, the creation of a finite element model is not the most ideal assessment tool of facial pressure distribution.

### **3.2.6 3D scanning techniques**

3D scanning techniques can be used to assess pressure distribution by aligning CAD models and creating colour map deviations [11]. These images provide useful visual information and mapping of areas of compression and relief. Reliable quantification of the actual pressure applied could not be determined.

# 4 Pilot study

Based on the results of the systematic review, a pilot study was performed to reach the aims described in section 1.2.

## 4.1 Methods and Materials

### 4.1.1 Design optimal workflow and prototype

One of our aims was to design the most optimal workflow for the fabrication process of facial pressure masks using 3D scanning and 3D printing techniques and to fabricate a prototype.

Based on expert opinions and the knowledge obtained from the systematic review, design requirements were defined in order to identify the most optimal fabrication workflow and to design a prototype according to this workflow. Pugh’s checklist was used to generate these requirements [60]. Different workflows were designed and compared based on these predefined requirements.

A prototype was fabricated for a healthy volunteer according to the most optimal workflow.

### 4.1.2 Validation

Two masks were fabricated for a healthy volunteer using two different moulds: (1) a 3D printed mould and (2) a conventional plaster mould.

A plaster impression was created by an experienced orthotist according to the conventional fabrication method described in section 2.5 (*Figure 7a*). A positive mould was created by filling the negative mould with plaster (*Figure 7b*). As no therapeutic pressure is desirable in this case, the orthotist adjusted the plaster mould with the aim to provide an even facial pressure distribution and avoid any pressure points.

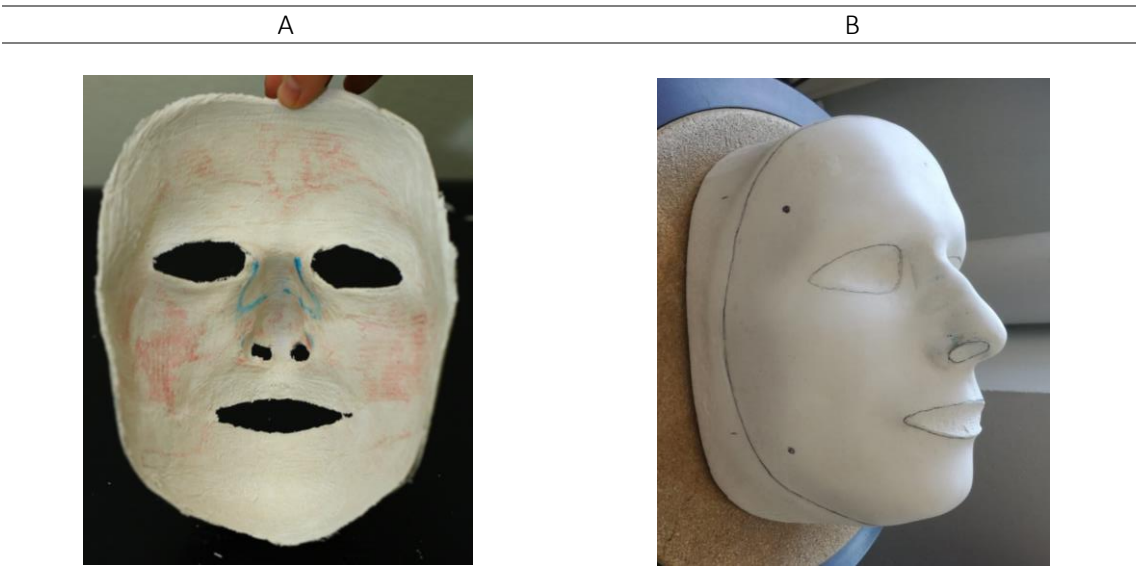


Figure 7 The conventional fabrication method of a positive plaster mould; a) A plaster impression was created by an experienced orthotist, resulting in a negative mould; b) A positive mould was created by filling the negative mould with liquid plaster. Manual adjustments were made with the aim to provide an even facial pressure distribution and avoid any pressure points.

It was not possible to complete the fabrication of a conventional facial mask on the healthy volunteer up to the fitting and delivery phase. Therefore, a 3D scan of the plaster mould was used to fabricate a facial mask that can be compared with a facial mask fabricated using a 3D scan of the face.

The masks were compared in terms of (1) comfort and (2) blanching of the skin as indirect measures for pressure distribution. From the assessment tools analyzed in section 3.2, the use of a 10-cm Visual Analogue Scale and digital imaging were identified as the most optimal tools.

Comfort levels were rated at the forehead, nasal bridge, chin and cheeks using the 10-cm Visual Analog Scale. The scale ranges from 0 to 10, where 0 represents no discomfort and 10 extreme discomfort. Digital imaging was used to visually check for any pressure points, characterized by blanching of the skin.

3D scanning techniques were used to create a colour map of the differences between the 3D scan of the face and the 3D scan of the positive plaster mould. In this way, manual adjustments made by the orthotist were visualized. These images were used to validate our findings.

Informed consent was obtained according to the Human Research Ethics guidelines.

## 4.2 Results

### 4.2.1 Design optimal workflow and prototype

#### 3D scanning

Design requirements are defined in order to design the most optimal workflow for the fabrication process of facial pressure masks using 3D scanning and printing techniques and to fabricate a prototype. The design requirements are presented in Appendix I.

Relevant requirements to identify the most optimal 3D scanning technique used to fabricate a facial pressure mask are:

- (1) The customized facial mask **shall not shift**.
- (2) The proposed fabrication method shall be **more comfortable** for the patient than the current fabrication method.
- (3) The proposed fabrication method of the customized facial mask shall be **less labour-intensive and more automated** than the current fabrication method.
- (4) *Wish*: the proposed fabrication method should **take less time** than the conventional fabrication method.
- (5) *Wish*: The customized facial mask should **not be more expensive** than the facial mask fabricated according to the conventional method.

As described in section 3.1.1, structured light and photogrammetry 3D scanners were available for use during this project. To fulfill requirement 1, accuracy is a decisive criteria on which the 3D scanners are assessed. To ensure accuracy, it is important to keep the head still during scanning. Therefore, speed is important as well. To fulfill requirements 2, 3 and 4, speed and ease-of-use are important factors. As a wish is to keep the costs as low as possible, purchase costs are compared as well. The comparison of available 3D scanners based on the predefined requirements is presented in *Table 3* [61]. A Harris profile was used to visualize the relative differences between the characteristics of the evaluated 3D scanners [62].

Table 3 A comparison of available 3D scanners based on predefined requirements. A Harris profile was used to visualize relative differences between the characteristics of the evaluated 3D scanners.

	Creaform Go!Scan 50				3dMD face				Artec Eva			
	--	-	+	++	--	-	+	++	--	-	+	++
Accuracy												
Speed												
Ease of use												
Costs												

While taking the important determinants into account, the Artec Eva (Artec 3D) appears to be the most appropriate 3D scanner for this application. This hand-held 3D scanner can capture the face in a few seconds with an accuracy up to 0.1 mm. Unfortunately, 3D scanners are expensive. The Artec Eva 3D scanner costs around €15.000. However, it could be cost-effective when used for several purposes in the hospital.

#### Computer aided design

After making an accurate 3D scan of the face, the digital model of the face can be exported from the Artec Eva software (Artec Studio 15, Artec 3D) to computer-aided-design software. Several CAD programs are suitable to design custom-made products.

Relevant requirements to identify the most optimal CAD software used to fabricate a facial pressure mask are:

- (1) The customized facial mask shall be **easy to adjust** during therapy.
- (2) The proposed fabrication method of the customized facial mask shall be **less labour-intensive and more automized** than the current fabrication method.
- (3) *Wish:* the proposed fabrication method should **take less time** than the conventional fabrication method.
- (4) *Wish:* The customized facial mask should **not be more expensive** than the conventional fabricated facial mask.

As described in section 3.1.2, Meshmixer (Autodesk) is easy-to-use free computer-aided-design software. While taking the important determinants into account, MeshMixer appears to be suitable for this application.

A 3D model of the face of a healthy individual acquired using 3D scanning can be seen in *Figure 8a*. A mask can be created based on this 3D scan using easy-to-use tools in Meshmixer (*Figure 8b*). As the orthotist uses the positive plaster mould to adjust the mask during therapy, the CAD model can be used as a mould in Meshmixer. The 3D model of the face and/or the designed mask can be easily adjusted by smoothly indenting or releasing the digital model.

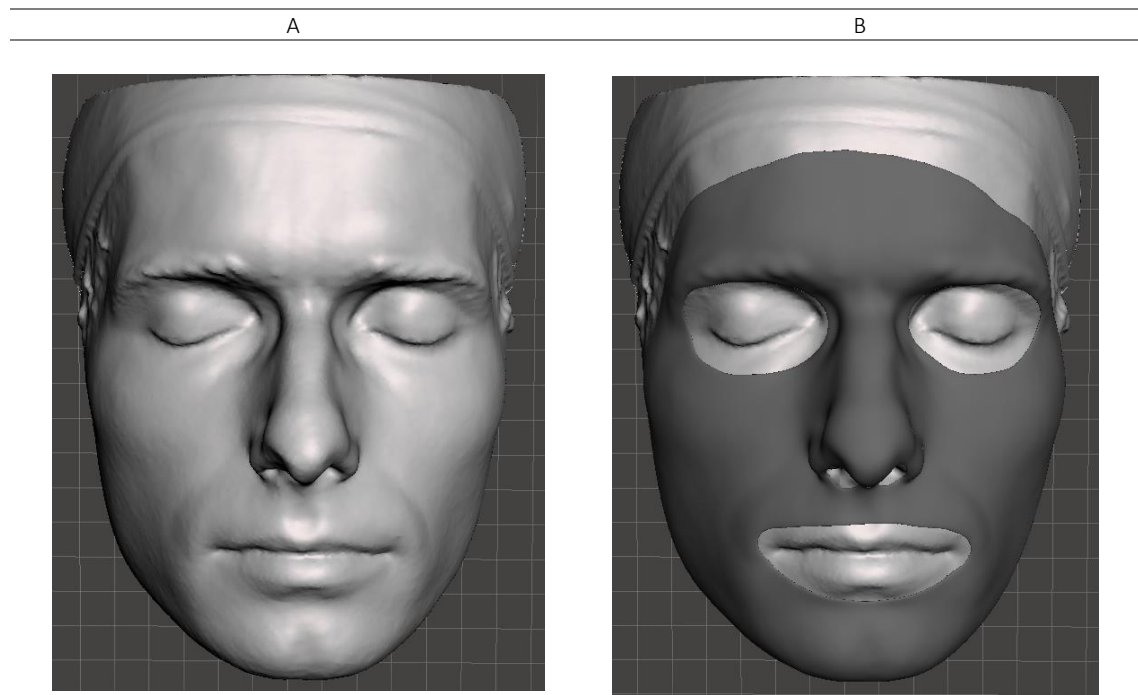


Figure 8 a) A 3D model of the face of a healthy volunteer acquired using 3D scanning; b) A facial mask designed In Meshmixer, using a 3D model of the face.

### 3D printing

After completion of the 3D design, a facial pressure mask can be fabricated using 3D printing techniques. Relevant requirements to identify the most optimal 3D printing technique(s) and materials used to fabricate the mask are:

- (1) The customized facial mask shall consist of a **medical-grade silicone lining** (Shore hardness 25-35 A). ISO10993 and USP Class VI biocompatibility certificates are needed.
- (2) The customized facial mask shall consist of a **rigid part** to apply pressure to the face.
- (3) The customized facial mask shall cover the **whole face**.
- (4) The customized facial mask shall be **transparent** because of aesthetics and monitoring of skin color (an appropriate parameter to establish the effects of applied pressure to the face).
- (5) The customized facial mask shall consist of **durable materials** that can be worn at least 12 hours a day, for a period of at least one year.
- (6) The customized facial mask shall be as **thin and light** as possible, while being **stable in shape**.
- (7) The customized facial mask shall be suitable for use under the following operating conditions:
  - a. Temperature: -20 to 60 degrees Celsius
  - b. Pressure: 15-40 mmHg (40 mmHg is the threshold for pressure ulcer formation)
- (8) The proposed fabrication method of the customized facial mask shall be **less labour-intensive and more automated** than the current fabrication method.
- (9) *Wish*: Parts and materials should be reusable or recyclable.
- (10) *Wish*: The proposed fabrication method should take **less time** than the conventional fabrication method.
- (11) *Wish*: The customized facial mask should **not be more expensive** than the conventional fabricated facial mask.

A conventional facial pressure mask consists of two transparent components: a rigid part and a medical-grade silicone lining. Based on the results of the literature review, it is not possible (yet) to print medical-grade silicones directly. Therefore, other alternatives are investigated to fabricate the silicone inner lining and to fulfill requirement (1).

As described in section 3.1.3, FDM and material jetting are available to print the rigid part of the facial mask during this project. In theory, 3D printing of a transparent rigid part of the right size is possible with these 3D printers. Transparent materials are evaluated in terms of (1) durability; (2) density; (3) strength; (4) printability; and (5) costs.

Suitable transparent materials are polylactic acid (PLA), acrylonitrile butadiene styrene (ABS), polyethylene terephthalate glycol (PETG), polycarbonate (PC) and Vero Ultra Clear (similar to polymethyl methacrylate, PMMA). All materials are recyclable.

The comparison of transparent 3D printing materials based on the predefined requirements is presented in *Table 4*. A Harris profile was used to visualize the relative differences between the characteristics of the evaluated materials [62].

Table 4 Comparison of 3D printing techniques and (transparent) materials in terms of durability, strength, printability, biodegradability and costs. A Harris profile is used to visualize relative differences between the characteristics of the evaluated materials (All3DP, 2020; CES EduPack, 2020).

	Fused Deposition Modeling																Material jetting			
	PLA				ABS				PET-G				PC				Vero Ultra Clear			
	--	-	+	++	--	-	+	++	--	-	+	++	--	-	+	++	--	-	+	++
Durability																				
Density																				
Strength																				
Printability																				
Costs																				

Based on this comparison, PET-G seems the most suitable material for a 3D printed facial mask. Therefore, a PET-G mask was printed at the Department of Experimental Instrumentation, Erasmus MC (DDDdrop Twin leader, DDDROP PETG clear, CAD2M). A 3D printed PET-G mask costs around €15.

In terms of transparency, the PET-G mask does not meet the requirements as it is not possible to monitor the skin through the mask (*Figure 9a*). A small sample of the nose was 3D printed using Vero Ultra Clear (*Figure 9b*). To 3D print a full-face mask, the costs are €700. Besides the fact that this material is expensive, it is not superior to PET-G in terms of transparency as well. By sanding and polishing the 3D printed mask, transparency could be enhanced. However, these extra steps are undesirable as one of the aims is to propose a workflow that is less labour-intensive and more automated than the current fabrication method.

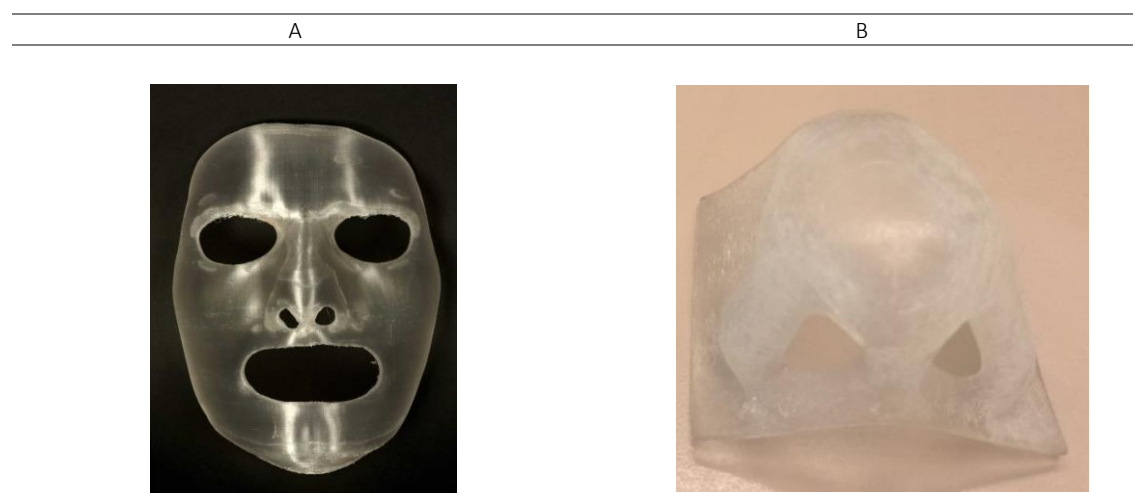


Figure 9 Comparison of 3D printed transparent materials. In terms of transparency, both materials do not meet the requirements as it is not possible to monitor the skin through the mask; a) A transparent PET-G mask; b) A Vero Ultra Clear sample.

As direct 3D printing of the medical-grade silicone lining is not possible yet and the direct 3D printed rigid part does not meet all predefined requirements, alternative workflows are investigated:

### Vacuum forming over a positive mould: an alternative to direct 3D printing

As outlined in section 3.1.3, Rogers et al. successfully investigated a fabrication process of a facial pressure mask using 3D scanning, milling and vacuum forming [49]. This process is presented as an appropriate alternative to 3D printing and is therefore investigated.

#### **Fabrication of the positive mould**

A positive mould can be fabricated based on a 3D scan using CNC foam milling, a subtractive manufacturing technique as described in section 3.1.3, or 3D printing.

It takes around 4 hours to fabricate a positive mould using CNC foam milling, whereas it takes more than 12 hours to fabricate a positive mould using 3D printing. However, the milling machine needs to be supervised at all times, while a 3D printer can print overnight. Furthermore, foam is relatively soft and can be easily damaged as can be seen in *Figure 10a*. For 3D printing, PLA can be used to fabricate a positive mould. As the heated sheet is in contact with the positive (thermoplastic) PLA mould for only a few seconds, the heat is not necessarily a concern [63] (*Figure 10b*). In case of spot-heating to adjust the thermoplastic mask during therapy, a more heat-resistant material is recommended, such as CPE+ (Ultimaker).

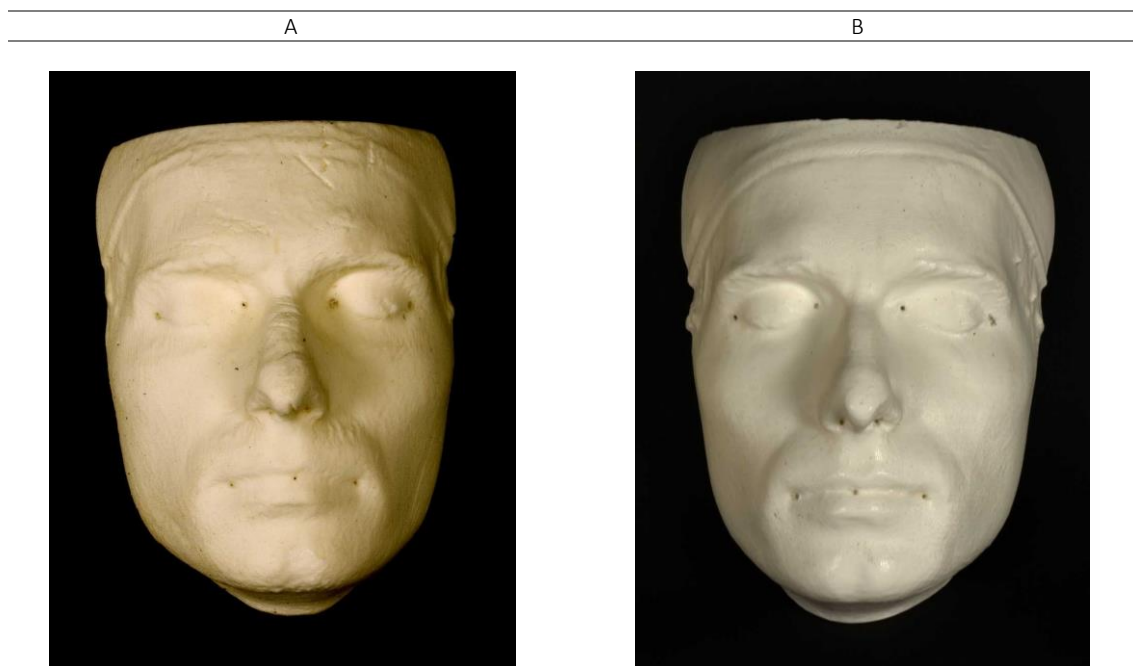


Figure 10 CNC foam milling compared with 3D printing (FDM) to fabricate a positive mould used for vacuum forming; a) The positive foam mould fabricated using CNC milling; b) The positive PLA mould fabricated using FDM printing.

#### **Vacuum forming**

Transparent thermoplastic sheets can be vacuum formed over a mould as an alternative to direct 3D printing of the rigid mask (with or without the silicone inner lining).

Vacuum forming, also called thermoforming, is a relatively easy process: A plastic sheet is heated to a pliable state. Once heated, a mould with the desired shape is forced against the sheet (*Figure 11*). The resulting model can be trimmed to create a usable product [63].

A promising material that can be vacuum formed over a positive mould is Silon-STs® (Bio Med Sciences, Inc., Allentown, PA), an orthotic material used to fabricate transparent facial pressure

masks and other scar management purposes [53, 64]. Silon-STS® is a Vivak® PET-G thermoplastic sheet with an adhered medical-grade silicone lining. The sheets are strong and light-weight with a thickness of 0.15 cm. One Silon®-STS sheet costs €165. The sheet can be spot-heated multiple times during therapy.

An alternative to the use of Silon®-STS is to fabricate the transparent rigid part and the silicone sheeting separately. The transparent rigid part can be made of Vivak® PET-G thermoplastic sheets with a thickness of 0.1 cm. Both Silon®-STS and Vivak® sheets can be rapidly vacuum formed at relatively low temperatures (120-160 °C). The medical-grade silicone inner lining can be fabricated by casting silicones in a 3D printed mould [65] or by rolling silicones using a two-roll mill [12]. However, these techniques are labour-intensive with long curing periods and are therefore not preferable.

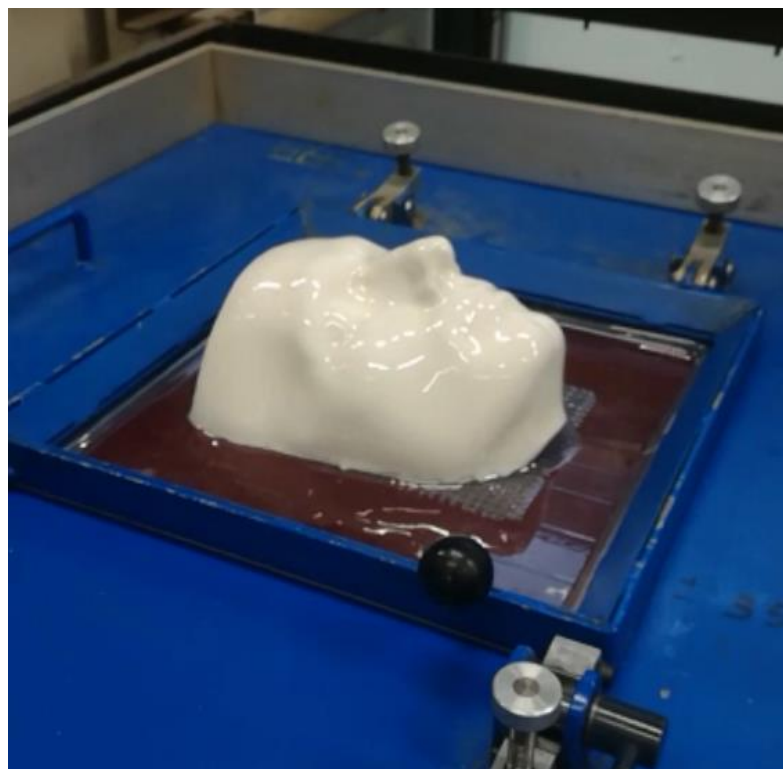


Figure 11 Vacuum forming of Silon-STS® over a 3D printed positive PLA mould

### Identification of the most optimal workflow

All (combinations of) evaluated fabrication methods outlined in section 4.2.1 are presented in *Figure 12*. To identify the most optimal workflow to fabricate facial pressure masks, all (combinations of) fabrication methods are compared with the traditional fabrication method.

Relevant requirements to identify the most optimal workflow are:

- (1) The proposed fabrication method of the customized facial mask shall be **less labour-intensive and more automatized** than the current fabrication method.
- (2) The proposed fabrication method shall be **more comfortable** for the patient than the current fabrication method.
- (3) *Wish*: The proposed fabrication method should take **less time** than the conventional fabrication method.
- (4) *Wish*: The customized facial mask should **not be more expensive** than the facial mask fabricated according to the conventional method

To fulfill these requirements, all workflows are compared in terms of (1) workload (man-hours, degree of automation and need for human expertise); (2) patient comfort; (3) total time; and (4) The results are presented in *Table 5*.

Based on the results presented in *Table 5*, workflow 5 seems the most optimal workflow in terms of total time, costs, workload (man-hours, degree of automation and need for human expertise) and patient comfort. This workflow consists of 3D scanning and 3D printing of a positive mould followed by vacuum forming of Silon-STS® over the positive mould. The most optimal workflow is shown in *Figure 13* (indicated in red).

This is a partly automated process that still needs human expertise. In theory, the proposed fabrication workflow is quicker and cheaper than the conventional method. The fabrication workflow including adjustments as part of the aftercare takes longer and is more expensive due to the fabrication of new positive moulds. However, the workflow contains the same number of man-hours as the conventional method in case of 8 iterations and patient comfort increases.

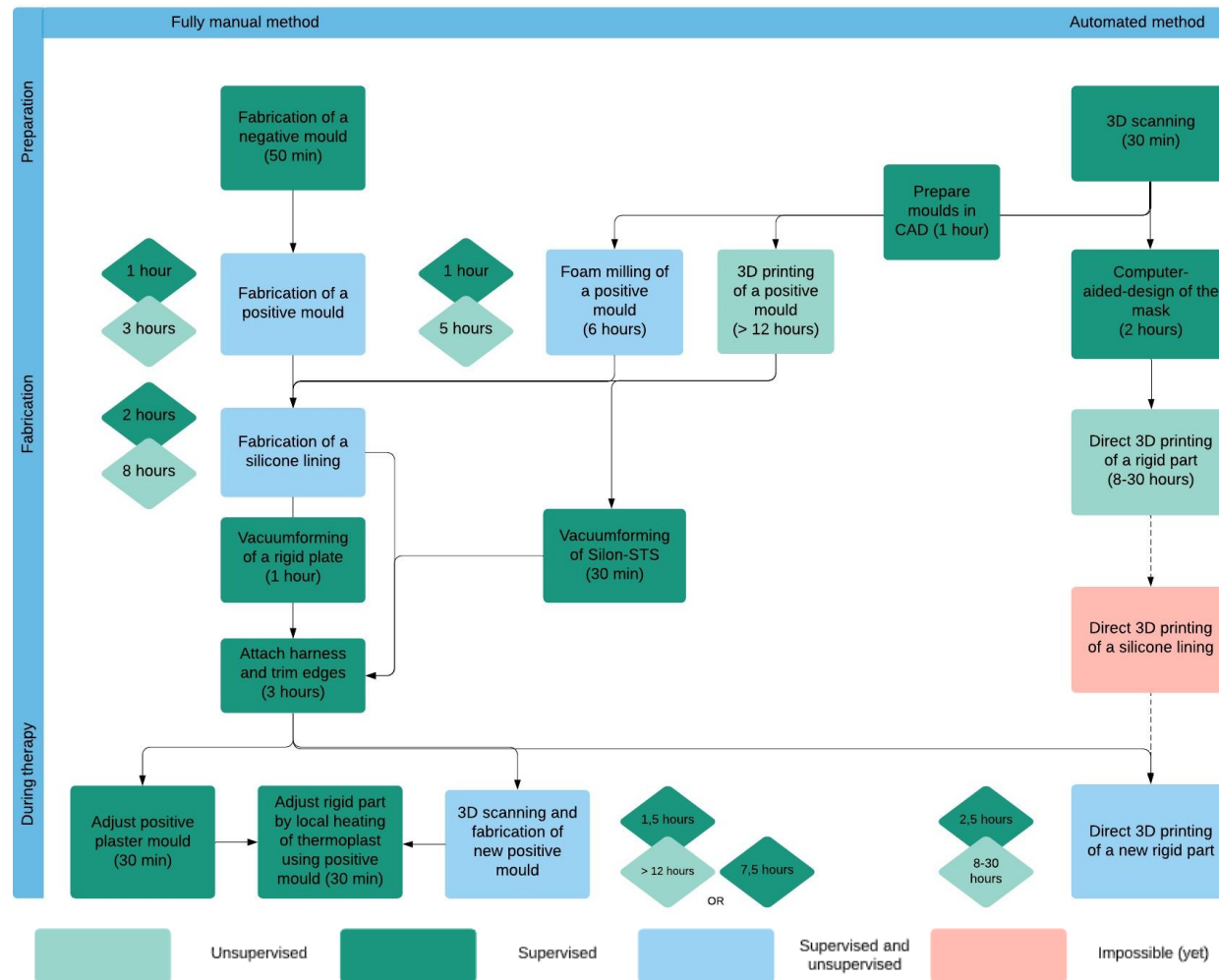





























Figure 12 An overview of all investigated workflows to fabricate a facial pressure mask with silicone sheeting, varying from the fully manual (conventional) fabrication method to an automated fabrication method including 3D scanning and 3D printing techniques.

Table 5 Comparison of workflows in terms of workload (man-hours, degree of automation and need for human expertise), patient comfort, total time and costs (including material and employee costs). Estimated material and employee costs are presented in Appendix II. A distinction is made between man-hours, total time and costs for 1 iteration, representing only the fabrication of the mask, and 8 iterations, representing fabrication including adjustments as part of the aftercare. The workflow indicated in grey represents the manual fabrication workflow as described by Colla et al. [12]. The workflow indicated in green represents the most optimal workflow in terms of the predefined variables. All workflows are presented in Appendix II.

	Man-hours (hours)		Degree of automation	Need for human expertise	Patient comfort	Total time (hours)		Costs (€)	
	1 iteration	8 iterations				1 iteration	8 iterations	1 iteration	8 iterations
Workflow 1	8	15				19	26	480	830
Workflow 2	9	30				22	78	505	1625
Workflow 3	8	18				28	126	455	1050
Workflow 4	6	27				11	67	490	1610
Workflow 5	5	19				17	115	440	1210
Workflow 6	10	31				31-53	87-109	545-1230	1665-2350
Workflow 7	9	23				37-59	135-1576	495-1180	1265-1950
Workflow 8	19	27				31-53	104-280	545-1230	1525-7005
Workflow 9	9	26				37-59	110-286	495-1180	1475-6955

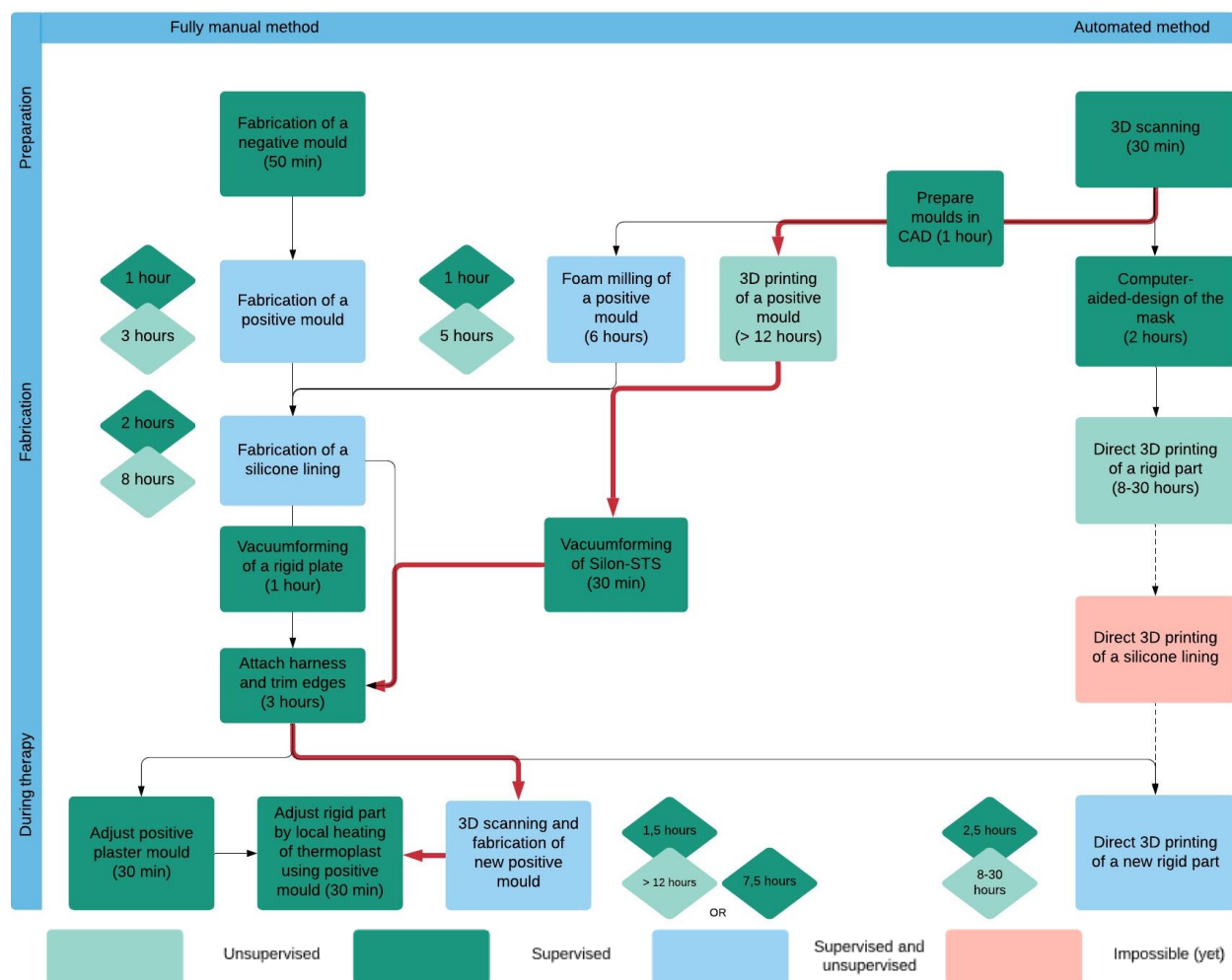


Figure 13 The most optimal workflow to fabricate facial pressure masks with a silicone sheeting using 3D scanning and 3D printing techniques (indicated in red). This workflow consists of 3D scanning, preparation of the positive mould in CAD, 3D printing of the positive (PLA) mould and vacuum forming of Silon-STS® over the positive mould.

### Fabrication of the prototype using 3D printing techniques

A prototype was fabricated for a healthy volunteer using 3D scanning and 3D printing techniques.

First, the 3D scan of the face, made with an Artec Eva 3D scanner, was converted as STL file. After removing any unnecessary details using MeshMixer, a positive PLA mould was 3D printed using an Ultimaker 2+ (Ultimaker). The mask was fabricated by vacuum forming a Silon®-STS sheet over a 3D printed positive PLA mould. After vacuum forming, it is important that the Silon®-STS material is quickly released and cooled by using compressed air.

Subsequently, the edges of the mask and holes around the mouth, nostrils and eyes were trimmed using a rotary tool. Five buckle anchors with nickel loops were attached to the mask. The healthy volunteer applied and fitted the mask (*Figure 14*). The elastic harness fabricated by an experienced orthotist was tightened to comfort and marked for consistent placement.

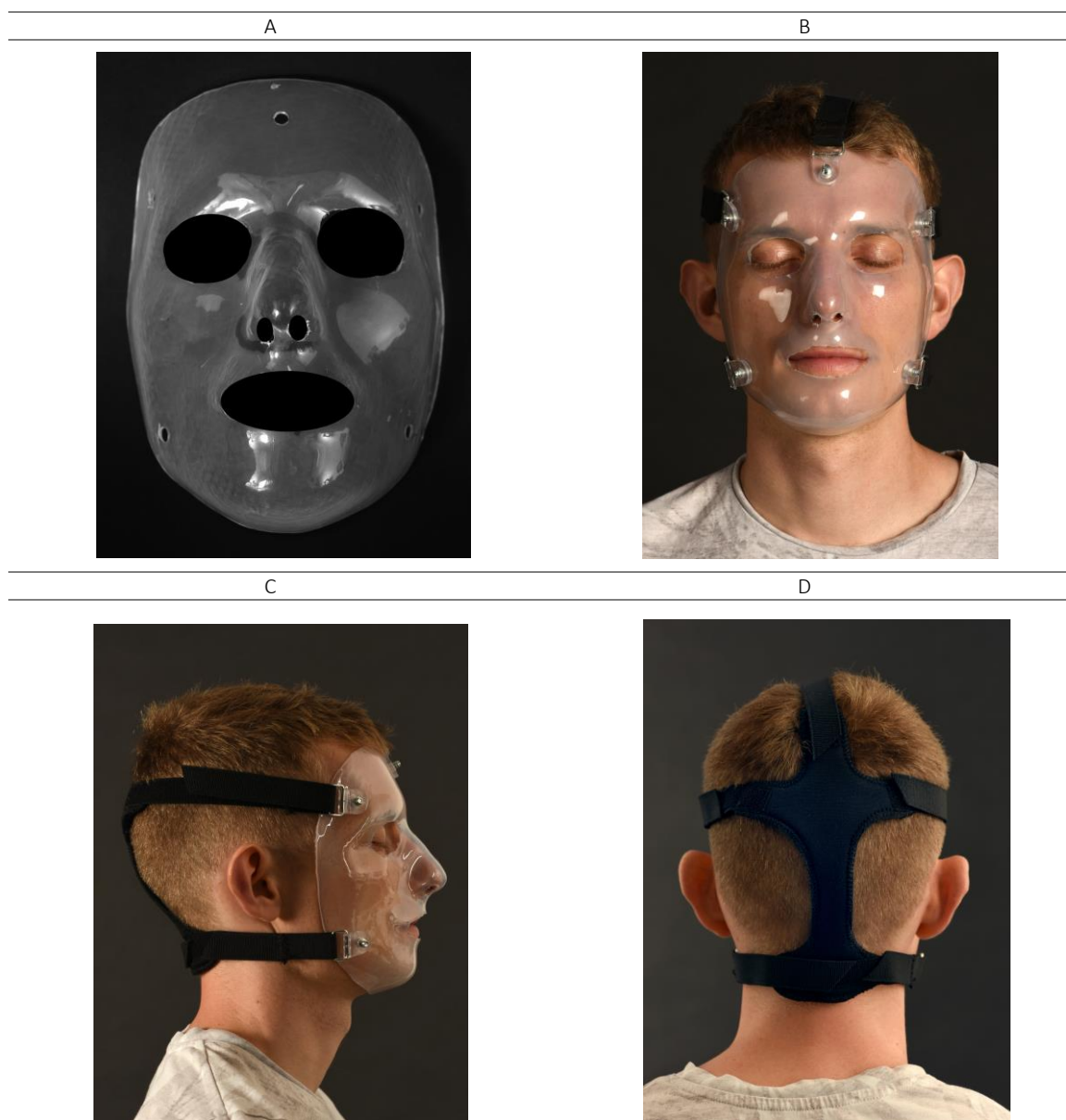


Figure 14 The prototype fabricated for a healthy volunteer using 3D scanning and 3D printing techniques; a) A prototype made of Silon-STS®, b) A healthy volunteer wearing the prototype (frontal view); c) A healthy volunteer wearing the prototype (lateral view); d) The elastic 5-point harness fabricated by an experienced orthotist.

### 4.2.2 Validation

Two masks were fabricated for a healthy volunteer using two different moulds: (1) a 3D printed mould and (2) a conventional plaster mould. Due to practical reasons, both masks were fabricated using Vivak® sheets (without silicone inner lining) instead of Silon-STs® for the assessment and comparison of facial pressure distribution. The masks were compared in terms of comfort and blanching of the skin as indirect measures for pressure distribution.

Comfort levels were rated at the forehead, nasal bridge, chin and cheeks using the 10-cm Visual Analogue Scale. The scale ranges from 0 to 10, where 0 represents no discomfort and 10 extreme discomfort. The results are presented in *Table 6*. Digital imaging was used to visually check for any pressure points, characterized by blanching of the skin.

Table 6 Comfort levels rated by the healthy volunteer for the masks fabricated using a 3D printed mould and a conventional plaster mould. The 10-cm Visual Analogue Scale was used to rate comfort levels. The scale ranges from 0 to 10, where 0 represents no discomfort and 10 extreme discomfort.

	3D scan of the face	Conventional plaster mould
Forehead	2	2
Nasal bridge	6	2
Left cheek	2	4
Right cheek	2	4
Chin	2	2

Overall, the facial mask that is fabricated using a 3D scan of the face and 3D printed mould is less comfortable than the mask fabricated using a conventional plaster mould. Especially at the nasal bridge increased pressure causes discomfort. In contrast, the facial mask fabricated using a plaster mould exerts more pressure on the cheeks, which results in higher discomfort levels.

Furthermore, digital imaging was used to visually check for any pressure points, characterized by blanching of the skin. These results are in accordance with the comfort levels scored by the healthy volunteer with the mask fabricated using a 3D scan of the face, because undesirable blanching of the skin is observed at the nasal bridge (*Figure 15*). No blanching of the skin is observed at the cheeks with the mask fabricated using a plaster mould, although discomfort is expressed.



Figure 15 Comparison of the two masks fabricated using a 3D scan of the face (A & C) and a conventional plaster mould (B & D) in terms of blanching of the skin as indirect measure for facial pressure distribution. Digital imaging was used to visually check for any pressure points, characterized by undesirable blanching of the skin. The mask fabricated using a 3D scan of the face causes undesirable blanching of the skin at the nasal bridge (indicated by orange arrow).

3D scanning techniques were used to quantify the differences between the 3D scan of the face and the 3D scan of the positive plaster mould. These differences were displayed by colour mapping. Artec Studio 12 (Artec 3D, Luxembourg) was used to align the two scans. In this way, manual adjustments made by the orthotist can be visualized. These images are used to validate our findings. The results are presented in Figure 16.

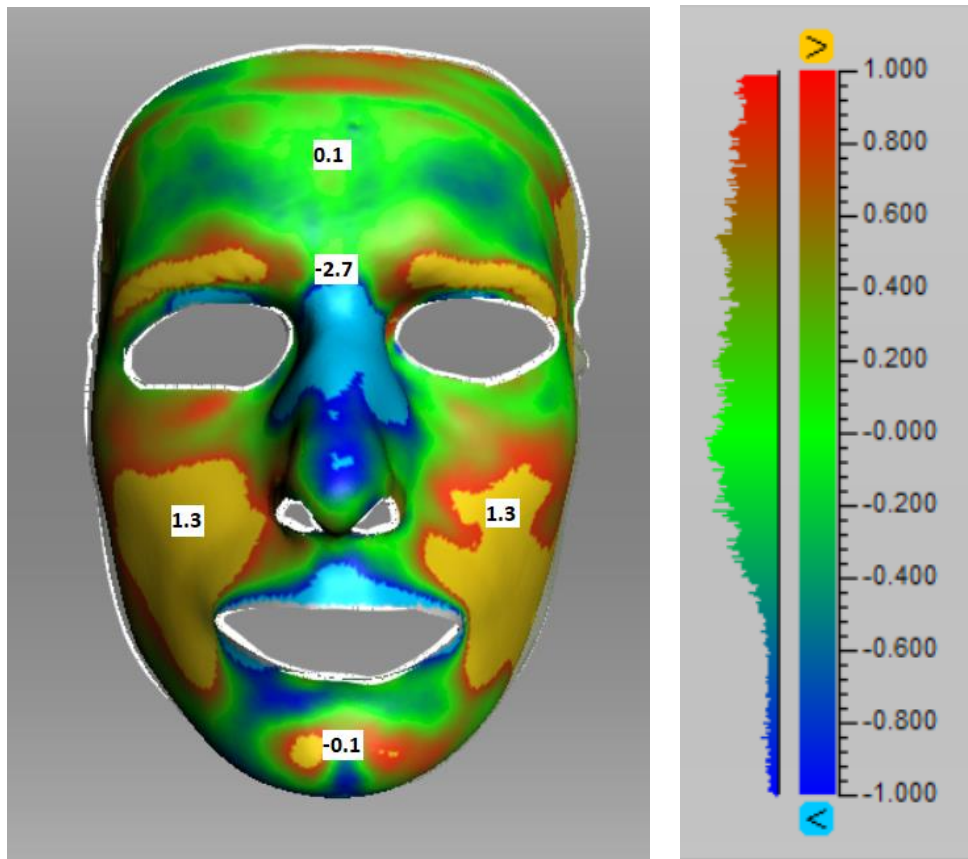


Figure 16 The 3D scan of the face relative to the 3D scan of the positive plaster mould. Red and yellow means that a mask fabricated using a conventional plaster mould will exert more pressure on the face, whereas blue areas signify that the mask fabricated using a plaster mould will exert less pressure on the face. Distances are expressed in millimeters (mm).

The results are in accordance with our observational findings that the facial mask fabricated using a plaster mould exerts less pressure on the nasal bridge and more pressure on the cheeks. As our healthy volunteer does not suffer from facial hypertrophic scarring, no blanching of the skin is desirable in this case. Moreover, discomfort should be absent in both cases. The facial mask fabricated based on a 3D scan causes blanching of the skin at the nasal bridge, but no discomfort in other areas. In contrast, the facial mask fabricated using a plaster mould does not cause blanching of the skin at the nose nor cheeks, but does not cause discomfort at the cheeks. Therefore, both masks need adjustments in case of clinical use.

# 5 Discussion

Medical applications for 3D scanning and 3D printing are rapidly expanding and are expected to revolutionize health care. Both 3D scanning and 3D printing are used to create customized medical devices, such as orthotics, prosthetics and implants [66] [67]. Therefore, it is hypothesized that these promising techniques can replace the current traditional fabrication process of facial pressure masks with silicone sheeting for patients with hypertrophic scars.

This systematic review and pilot study show that it is not possible yet to 3D print all components of the mask, and therefore the proposed workflow consists of both manual and automated steps. Moreover, digital design modifications are needed to further optimize the prototype presented to provide adequate pressure therapy.

## 3D technology

We conclude that the most promising workflow to fabricate facial pressure masks with silicone sheeting using 3D technology consists of 3D scanning of the face, 3D printing of a positive mould and vacuum forming of Silon®-STS thermoplastic sheets with silicone inner lining over the positive mould.

Previous research on 3D printed facial masks is scarce. Wei et al. investigated the use of direct 3D printed facial masks in the treatment of facial hypertrophic scars of young children due to burns [16]. Since direct 3D printing of medical-grade silicones is not possible yet, layers of silicone gel were lined on the inside surface of the facial mask. A limitation of the study is that the fabrication of only one 3D printed mask is up to three times more expensive than the traditional fabrication method. In our study, the proposed fabrication method using 3D printing techniques is affordable, while eliminating the plaster mould taking procedures as well.

During this study, the first step towards a digital fabrication workflow is presented. The most optimal workflow identified during this study is based on the results of the systematic review and first tests with one healthy volunteer. Future research should investigate the suitability of the proposed workflow for more healthy volunteers before use in a clinical setting. The ultimate goal is to set up a clinical comparative study on patients after oncological facial reconstructions.

## Facial pressure distribution

Our findings that digital design modifications are needed prior to 3D printing of the positive mould are in line with previous research. Wei et al. described the use of finite element modeling to show that a facial mask designed without geometric modifications results in an imbalance of pressure distribution [17].

Wei et al. and Pilley et al. outlined that these modifications still need to be performed manually by an experienced orthotist or prosthetist, either digital or using a plaster mould [17, 58]. Since we aim for a digital fabrication workflow that is more automatized than the current fabrication workflow, future research should focus on the integration of tools to automate these (digital) modifications.

Allely et al. and Van-Buendia et al. mentioned that Laser Doppler Imaging may prove to be valuable to quantify the pressure produced by the facial masks. Allely et al. investigated that LDI can measure perfusion at high percent pixel validity through a transparent facial mask. This finding implies that LDI can be used to objectively determine the efficacy of pressure by evaluating perfusion in hypertrophic scars. However, further research into its applicability is needed and LDI was not available during our study

Due to the fact that there are no reliable (integrated) pressure sensors yet, pressure distribution was assessed indirectly in this study. As it is desirable to monitor the pressure applied by the facial mask directly and continuously, developments in the field of thin pressure sensors should be given close attention in the future. When pressure applied by the facial mask can be measured directly and continuously with pressure sensors, the effect of the treatment can be assessed more objectively. Moreover, outcomes might be evaluated with the use of video consultations, which potentially reduces the high costs of aftercare.

## Validation

To our knowledge, this is the first study that investigated the differences between a facial mask fabricated using a handmade plaster mould and a facial mask fabricated using 3D scanning and printing techniques in terms of the manufacturing process and facial pressure distribution.

Several remarks can be made with regard to this validation method. It was not possible to complete the fabrication of a conventional facial mask made by an experienced orthotist. Since the conventional facial mask is considered the 'gold standard', ideally this conventional mask was compared to the preliminary prototype fabricated in this study. Furthermore, the location of buckle anchors attached to the facial masks might have differed slightly due to differences in geometry between the moulds. This could have affected the results.

## Clinical implications

To date, not every patient with facial hypertrophic scarring eligible for treatment with a silicone facial pressure mask, can be treated. This is due to the fact that an experienced and dedicated orthotist is needed for the fabrication process of these masks. The MUMC+ is the only place in the Netherlands where such an orthotist is employed. As the number of patients with facial hypertrophic scarring due to the rising numbers of skin cancer is increasing, a more automated workflow for the fabrication of these facial masks is desirable. In this way, non-invasive treatment of facial hypertrophic scars by a silicone facial pressure mask can be offered to more patients. This could improve outcomes and/or prevent patients from surgical correction of the scars.

Since further optimization and validation of the proposed workflow is needed, future research should focus on digital modification of the mask and more objective pressure measurement tools.

A research direction that can be explored is the generation of a system based on clustering. In close collaboration with experienced orthotists, healthy volunteers can be categorized into groups with corresponding facial features. This system may serve as a basis to automate digital modifications needed for adequate pressure therapy.

As the burden of wearing a full-face pressure mask should not be underestimated, future research should focus on the optimization of the facial mask design to improve comfort and reduce excessive sweating. In this way, patient compliance could be increased.

Furthermore, facial 3D scanning can be used to closely monitor the effect of the treatment by comparing 3D scans acquired during the treatment period. Showing these results to the patient could help improve compliance as well.

Future goals in a clinical setting will be to evaluate (1) cost-effectiveness; (2) long-term clinical effects in patients and (3) patient reported outcome measures.

## 6 Conclusion

Based on our preliminary results, 3D technology seems suitable to partly replace the traditional fabrication method of transparent facial pressure masks for the treatment of hypertrophic scarring.

In this study, the most optimal workflow using 3D technology is presented. This workflow consists of both manual and automated steps.

To further optimize and validate the proposed workflow, future research should focus on digital modification of the mask and more objective pressure measurement tools.

# References

1. Bock, O., et al., *Quality of life of patients with keloid and hypertrophic scarring*. Arch Dermatol Res, 2006. **297**(10): p. 433-8.
2. Gibson, J.A.G., et al., *The association of affective disorders and facial scarring: Systematic review and meta-analysis*. J Affect Disord, 2018. **239**: p. 1-10.
3. Gauglitz, G.G., et al., *Hypertrophic scarring and keloids: pathomechanisms and current and emerging treatment strategies*. Mol Med, 2011. **17**(1-2): p. 113-25.
4. Van den Kerckhove, E., et al., *The assessment of erythema and thickness on burn related scars during pressure garment therapy as a preventive measure for hypertrophic scarring*. Burns, 2005. **31**(6): p. 696-702.
5. Anthonissen, M., et al., *The effects of conservative treatments on burn scars: A systematic review*. Burns, 2016. **42**(3): p. 508-18.
6. Van den Kerckhove, E., et al., *Silicones in the rehabilitation of burns: a review and overview*. Burns, 2001. **27**(3): p. 205-14.
7. Steinstraesser, L., et al., *Pressure garment therapy alone and in combination with silicone for the prevention of hypertrophic scarring: randomized controlled trial with intraindividual comparison*. Plast Reconstr Surg, 2011. **128**(4): p. 306e-313e.
8. Li-Tsang, C.W., Y.P. Zheng, and J.C. Lau, *A randomized clinical trial to study the effect of silicone gel dressing and pressure therapy on posttraumatic hypertrophic scars*. J Burn Care Res, 2010. **31**(3): p. 448-57.
9. Rivers, E.A., R.G. Strate, and L.D. Solem, *The transparent face mask*. Am J Occup Ther, 1979. **33**(2): p. 108-13.
10. Kant, S.B., et al., *Clinical effects of transparent facial pressure masks: A literature review*. Prosthet Orthot Int, 2019. **43**(3): p. 349-355.
11. Parry, I., et al., *Harnessing the Transparent Face Orthosis for facial scar management: a comparison of methods*. Burns, 2013. **39**(5): p. 950-6.
12. Colla, C., et al., *Manual fabrication of a specialized transparent facial pressure mask: A technical note*. Prosthet Orthot Int, 2019. **43**(3): p. 356-360.
13. Singleterry, J.J.W., DC: The Cost of Cancer, *The Cost of Cancer: Addressing Patient Costs (American Cancer Society Cancer Action Network)*. 2017.
14. Lomas, A., J. Leonardi-Bee, and F.J.B.J.o.D. Bath-Hextall, *A systematic review of worldwide incidence of nonmelanoma skin cancer*. 2012. **166**(5): p. 1069-1080.
15. Hollestein, L.M., et al., *Burden of disease caused by keratinocyte cancer has increased in The Netherlands since 1989*. 2014. **71**(5): p. 896-903.
16. Wei, Y., et al., *3D-printed transparent facemasks in the treatment of facial hypertrophic scars of young children with burns*. Burns, 2017. **43**(3): p. e19-e26.
17. Wei, Y., et al., *The application of 3D-printed transparent facemask for facial scar management and its biomechanical rationale*. Burns, 2018. **44**(2): p. 453-461.
18. Reinke, J.M. and H. Sorg, *Wound Repair and Regeneration*. European Surgical Research, 2012. **49**(1): p. 35-43.
19. Xue, M. and C.J.J.A.i.w.c. Jackson, *Extracellular matrix reorganization during wound healing and its impact on abnormal scarring*. 2015. **4**(3): p. 119-136.
20. Baum, C.L. and C.J.J.D.s. Arpey, *Normal cutaneous wound healing: clinical correlation with cellular and molecular events*. 2005. **31**(6): p. 674-686.
21. Ogawa, R., *Keloid and Hypertrophic Scars Are the Result of Chronic Inflammation in the Reticular Dermis*. Int J Mol Sci, 2017. **18**(3).
22. Van Loey, N.E.E., et al., *Itching following burns: epidemiology and predictors*. 2008. **158**(1): p. 95-100.

23. Bell, L., et al., *Pruritus in burns: a descriptive study*. 1988. **9**(3): p. 305.
24. Wheeland, R., *Cutaneous Medicine and Surgery*. 1996.
25. Alster, T.S. and T.B.J.A.o.p.s. West, *Treatment of scars: a review*. 1997. **39**: p. 418-432.
26. Deitch, E.A., et al., *Hypertrophic burn scars: analysis of variables*. J Trauma, 1983. **23**(10): p. 895-8.
27. Lewis, W.H. and K.K. Sun, *Hypertrophic scar: a genetic hypothesis*. Burns, 1990. **16**(3): p. 176-8.
28. Butzelaar, L., et al., *Currently known risk factors for hypertrophic skin scarring: A review*. J Plast Reconstr Aesthet Surg, 2016. **69**(2): p. 163-9.
29. Ho, T. and P.J. Byrne, *Evaluation and initial management of the patient with facial skin cancer*. Facial Plast Surg Clin North Am, 2009. **17**(3): p. 301-7.
30. Connolly, S.M., et al., *AAD/ACMS/ASDSA/ASMS 2012 appropriate use criteria for Mohs micrographic surgery: a report of the American Academy of Dermatology, American College of Mohs Surgery, American Society for Dermatologic Surgery Association, and the American Society for Mohs Surgery*. J Am Acad Dermatol, 2012. **67**(4): p. 531-50.
31. Meaie, J.D., et al., *Facial Skin Cancer Reconstruction*. Semin Plast Surg, 2016. **30**(3): p. 108-21.
32. Levine, E., et al., *Quality of life and facial trauma: psychological and body image effects*. 2005. **54**(5): p. 502-510.
33. Macintyre, L. and M.J.B. Baird, *Pressure garments for use in the treatment of hypertrophic scars—a review of the problems associated with their use*. 2006. **32**(1): p. 10-15.
34. Stewart, R., et al., *Pressure garment adherence in adult patients with burn injuries: an analysis of patient and clinician perceptions*. Am J Occup Ther, 2000. **54**(6): p. 598-606.
35. Gottfried Medical, I. *Custom Compression Therapy: Face Masks and Chin Straps*. 2020; Available from: <https://www.gottfriedmedical.com/custom-compression-garments/face-masks-chin-straps/face-masks-chin-straps.php>.
36. Sand, M., et al., *Combination of surgical excision and custom designed silicon pressure splint therapy for keloids on the helical rim*. Head & face medicine, 2007. **3**: p. 14.
37. Koudougou, C., et al., *Conception and use of a custom-made facial mask for pressure therapy in complex facial wounds*. J Stomatol Oral Maxillofac Surg, 2019.
38. Mustoe, T.A.J.A.p.s., *Evolution of silicone therapy and mechanism of action in scar management*. 2008. **32**(1): p. 82.
39. Slem, A.E. and R.E. Kirschner, *Keloids and scars: a review of keloids and scars, their pathogenesis, risk factors, and management*. Curr Opin Pediatr, 2006. **18**(4): p. 396-402.
40. Kloeters, O., A. Tandara, and T.A. Mustoe, *Hypertrophic scar model in the rabbit ear: a reproducible model for studying scar tissue behavior with new observations on silicone gel sheeting for scar reduction*. Wound Repair Regen, 2007. **15** Suppl 1: p. S40-5.
41. Tandara, A.A. and T.A. Mustoe, *The role of the epidermis in the control of scarring: evidence for mechanism of action for silicone gel*. J Plast Reconstr Aesthet Surg, 2008. **61**(10): p. 1219-25.
42. Suetak, T., et al., *Effects of silicone gel sheet on the stratum corneum hydration*. Br J Plast Surg, 2000. **53**(6): p. 503-7.
43. Monstrey, S., et al., *Updated Scar Management Practical Guidelines: Non-invasive and invasive measures*. Journal of Plastic, Reconstructive & Aesthetic Surgery, 2014. **67**(8): p. 1017-1025.
44. Koc, E., et al., *An open, randomized, controlled, comparative study of the combined effect of intralesional triamcinolone acetonide and onion extract gel and intralesional triamcinolone acetonide alone in the treatment of hypertrophic scars and keloids*. 2008. **34**(11): p. 1507-1514.
45. Juckett, G. and H. Hartman-Adams, *Management of keloids and hypertrophic scars*. Am Fam Physician, 2009. **80**(3): p. 253-60.
46. Lewis, D. and D.J.T.J.o.p.d. Castleberry, *An assessment of recent advances in external maxillofacial materials*. 1980. **43**(4): p. 426-432.
47. Narayan, K.L., *Computer Aided Design and Manufacturing*. 2008, New Delhi: Prentice Hall of India.

48. 3Dnatives. *3D Printing vs CNC Machining: Which is best for prototyping?* 2018; Available from: <https://www.3dnatives.com/en/3d-printing-vs-cnc-160320184/#:~:text=They%20key%20difference%20between%203D,whilst%20CNC%20machining%20is%20subtractive.&text=Some%20advantages%20of%20CNC%20machining,wood%2C%20metals%20and%2C%20plastics.>
49. Rogers, B., et al., *Computerized manufacturing of transparent face masks for the treatment of facial scarring*. 2003. **24**(2): p. 91-96.
50. Shikama, M., et al., *Development of personalized fitting device with 3-dimensional solution for prevention of niv oronasal mask-related pressure ulcers*. *Respir Care*, 2018. **63**(8): p. 1024-1032.
51. Melia, M., et al., *Pressure pain thresholds: Subject factors and the meaning of peak pressures*. *Eur J Pain*, 2019. **23**(1): p. 167-182.
52. Lai, C.H.Y. and C.W.P. Li-Tsang, *Validation of the Pliance X System in measuring interface pressure generated by pressure garment*. *Burns*, 2009. **35**(6): p. 845-851.
53. Allely, R.R., et al., *Laser doppler imaging of cutaneous blood flow through transparent face masks: A necessary preamble to computer-controlled rapid prototyping fabrication with submillimeter precision*. *J Burn Care Res*, 2008. **29**(1): p. 42-48.
54. Hop, M.J., et al., *Cost-effectiveness of laser doppler imaging in burn care in The Netherlands: a randomized controlled trial*. 2016. **137**(1): p. 166e-176e.
55. Yamamoto, T., et al., *Derivation and clinical application of special imaging by means of digital cameras and Image J freeware for quantification of erythema and pigmentation*. *Skin Res Technol*, 2008. **14**(1): p. 26-34.
56. Worsley, P.R., et al., *Investigating the effects of strap tension during non-invasive ventilation mask application: A combined biomechanical and biomarker approach*. *Med Devices Evid Res*, 2016. **9**: p. 409-417.
57. Powell, B.W., C. Haylock, and J.A. Clarke, *A semi-rigid transparent face mask in the treatment of postburn hypertrophic scars*. *Br J Plast Surg*, 1985. **38**(4): p. 561-6.
58. Pilley, M.J., et al., *The use of non-contact structured light scanning in burns pressure splint construction*. *Burns*, 2011. **37**(7): p. 1168-1173.
59. Cai, M., et al., *Customized design and 3D printing of face seal for an N95 filtering facepiece respirator*. *J Occup Environ Hyg*, 2018. **15**(3): p. 226-234.
60. Pugh, S., *Integrated methods for successful product engineering*. 1990: Addison-Wesley.
61. ANIWAA. *3D scanners comparison*. 2020; Available from: <https://www.aniwaa.com/comparison/3d-scanners/>.
62. Harris, J.S., *The Product Profile Chart: A Graphical Means of Appraising and Selecting New Products*. 1961.
63. Makerbot Industries, I. *How to vacuumform using 3D printed moulds*. 2020; Available from: <https://www.makerbot.com/professional/post-processing/vacuum-forming/>.
64. Van-Buendia, L.B., et al., *What's behind the mask? A look at blood flow changes with prolonged facial pressure and expression using laser doppler imaging*. *J Burn Care Res*, 2010. **31**(3): p. 441-447.
65. Visscher, D.O., et al., *3D printing of patient-specific neck splints for the treatment of post-burn neck contractures*. *Burns Trauma*, 2018. **6**: p. 15.
66. Haleem, A., M.J.C.E. Javaid, and G. Health, *3D scanning applications in medical field: a literature-based review*. 2019. **7**(2): p. 199-210.
67. Ventola, C.L., *Medical Applications for 3D Printing: Current and Projected Uses*. P t, 2014. **39**(10): p. 704-11.

# Appendices

## Appendix I Design requirements

The list is based on the analysis phase of this thesis and Pugh's checklist:

### Requirements for the facial mask

#### **Performance and fabrication**

- (1) The customized facial mask shall apply a facial pressure distribution of less than 15 mmHg on healthy skin and between 15 and 40 mmHg on scar tissue.
- (2) The customized facial mask shall consist of a medical-grade silicone lining (Shore hardness 25-35 A [46]). ISO10993 and USP Class VI biocompatibility certificated are needed.
- (3) The customized facial mask shall consist of a rigid part to apply pressure to the face.
- (4) The customized facial mask shall not shift.
- (5) The customized facial mask shall consist of durable materials that can be worn at least 12 hours a day, for a period of at least one year.
- (6) The customized facial mask shall be easy to adjust during therapy.
- (7) The proposed fabrication method shall be more comfortable for the patient than the current fabrication method.
- (8) The proposed fabrication method of the customized facial mask shall be less labour-intensive and more automated than the current fabrication method.

#### **Environment**

- (9) The customized facial mask shall be suitable for use under the following operating conditions:
  - a. Temperature: -20 to 60 degrees Celsius
  - b. Pressure: 15-40 mmHg (40 mmHg is the threshold for pressure ulcer formation)

#### **Maintenance**

- (10) The headgear shall be hand or machine washable to reduce the amount of disposed headgears.
- (11) The customized facial mask shall be easily cleaned using suitable cleaning techniques.

#### **Geometry**

- (12) The customized facial mask shall be as thin and light as possible, while being stable in shape.
- (13) The customized facial mask shall be attached to the face by an adjustable harness.

#### **Aesthetic, Appearance and Finish**

- (14) The customized facial mask shall be transparent because of aesthetics and monitoring of skin colour (an appropriate parameter to establish the effects of applied pressure to the face).
- (15) The customized facial mask shall be smoothly finished.

### **Safety**

- (16) The customized facial mask shall not impair breathing.
- (17) The harness shall be easily attached and removed.

### **Wishes**

- (18) The customized facial mask should consist of as few components as possible.
- (19) Parts and materials should be reusable or recyclable.
- (20) The proposed fabrication method should take less time than the conventional fabrication method.
- (21) The customized facial mask should not be more expensive than the conventional fabricated facial mask.

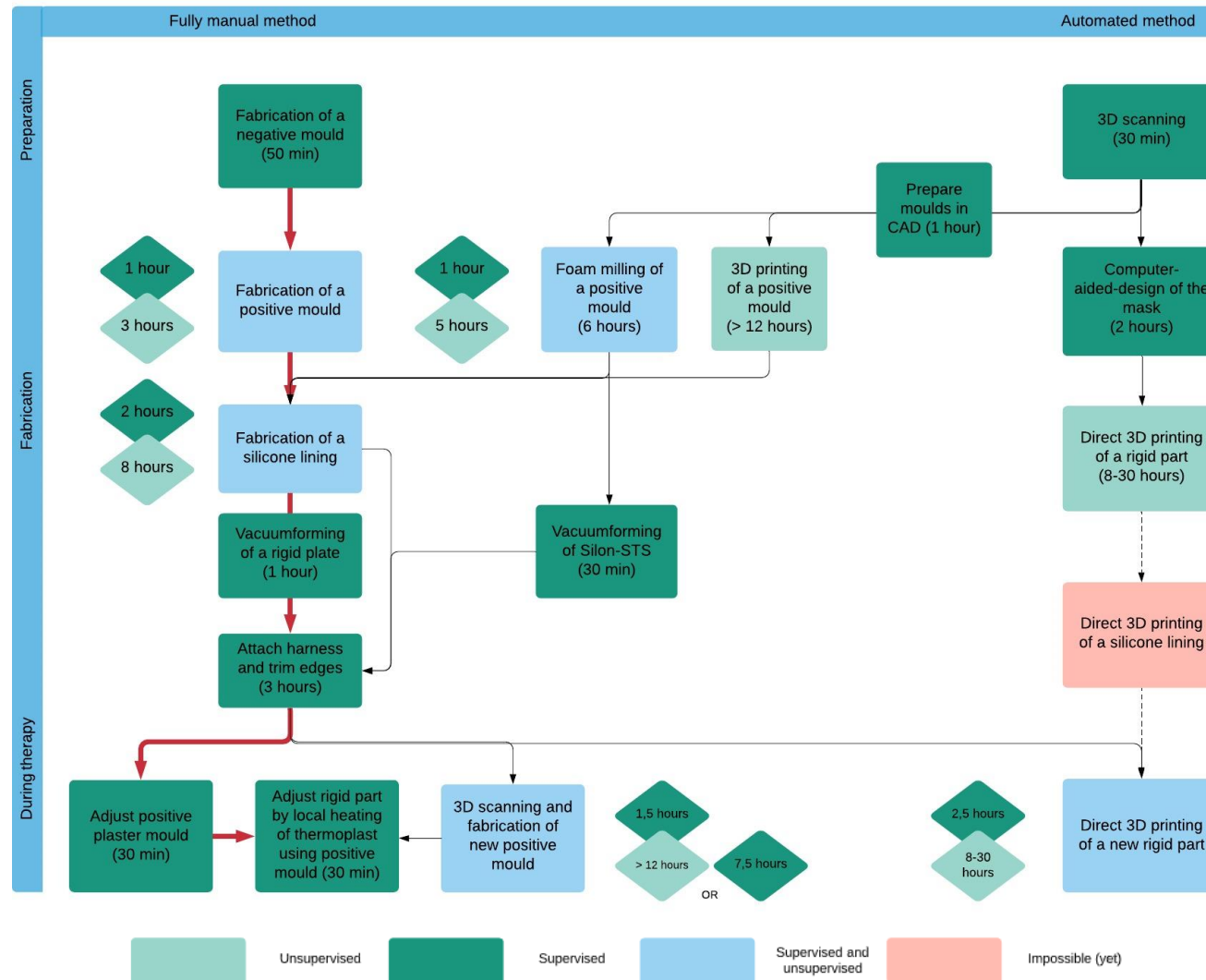
## Appendix II Workflows

An overview of estimated costs, used to identify the most optimal workflow, is presented in *Table 7*. All workflows presented in section 4.2.1, ranging from a fully manual to an automated workflow, are visualized in this Appendix.

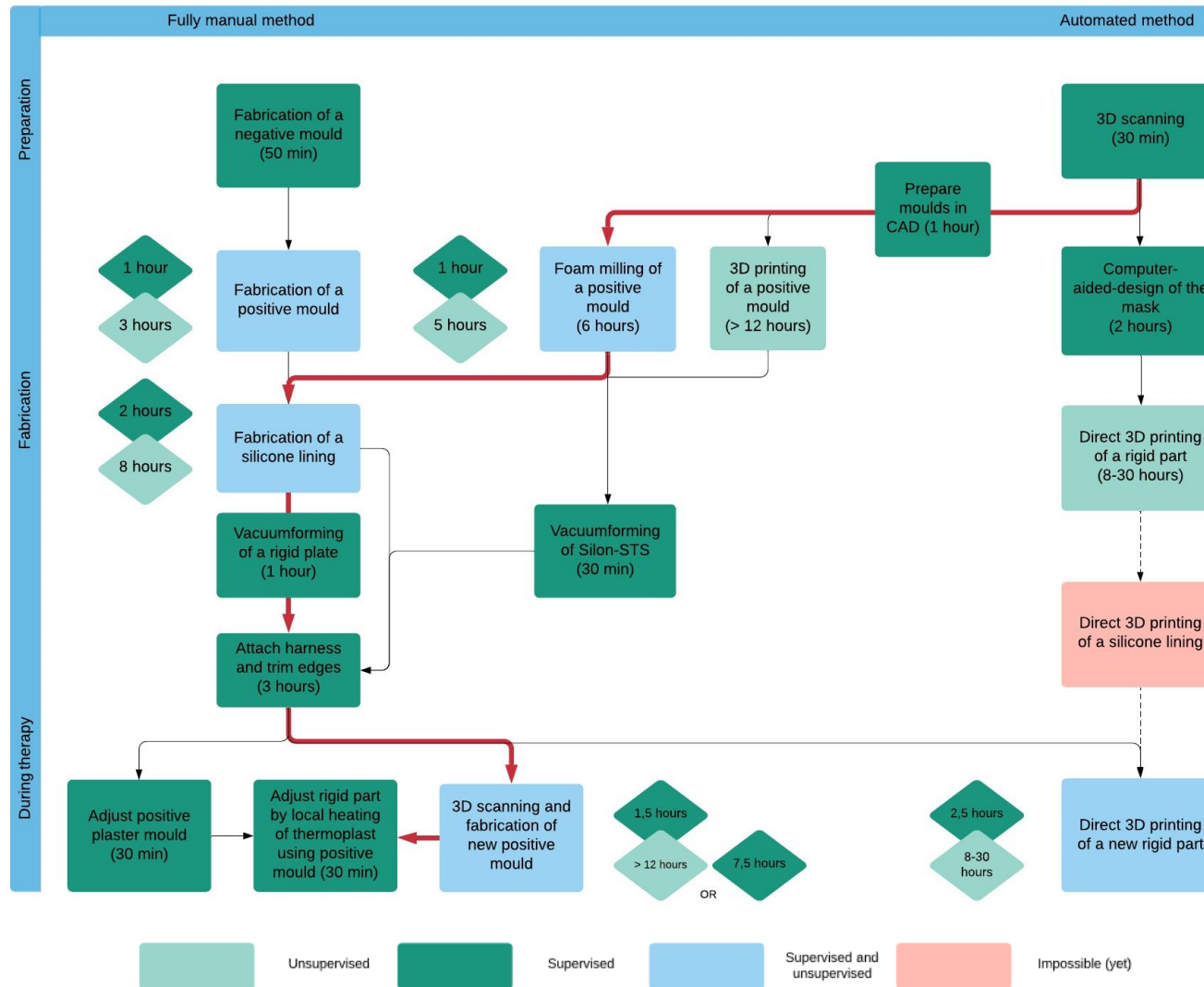
Table 7 An overview of estimated costs, used to identify the most optimal workflow.

Estimated costs	€
Fabrication of a negative mould	10
Fabrication of a positive mould	10
Fabrication of a silicone inner lining	30
Vacuumforming of a rigid plate	25
Attach harness and trim edges	15
Foam milling of a positive mould	10
3D printing of a positive mould	10
Vacuumforming of Silon-STS®	165
Direct 3D printing of a rigid part	15-700
Employee (experienced orthotist)	50/hour

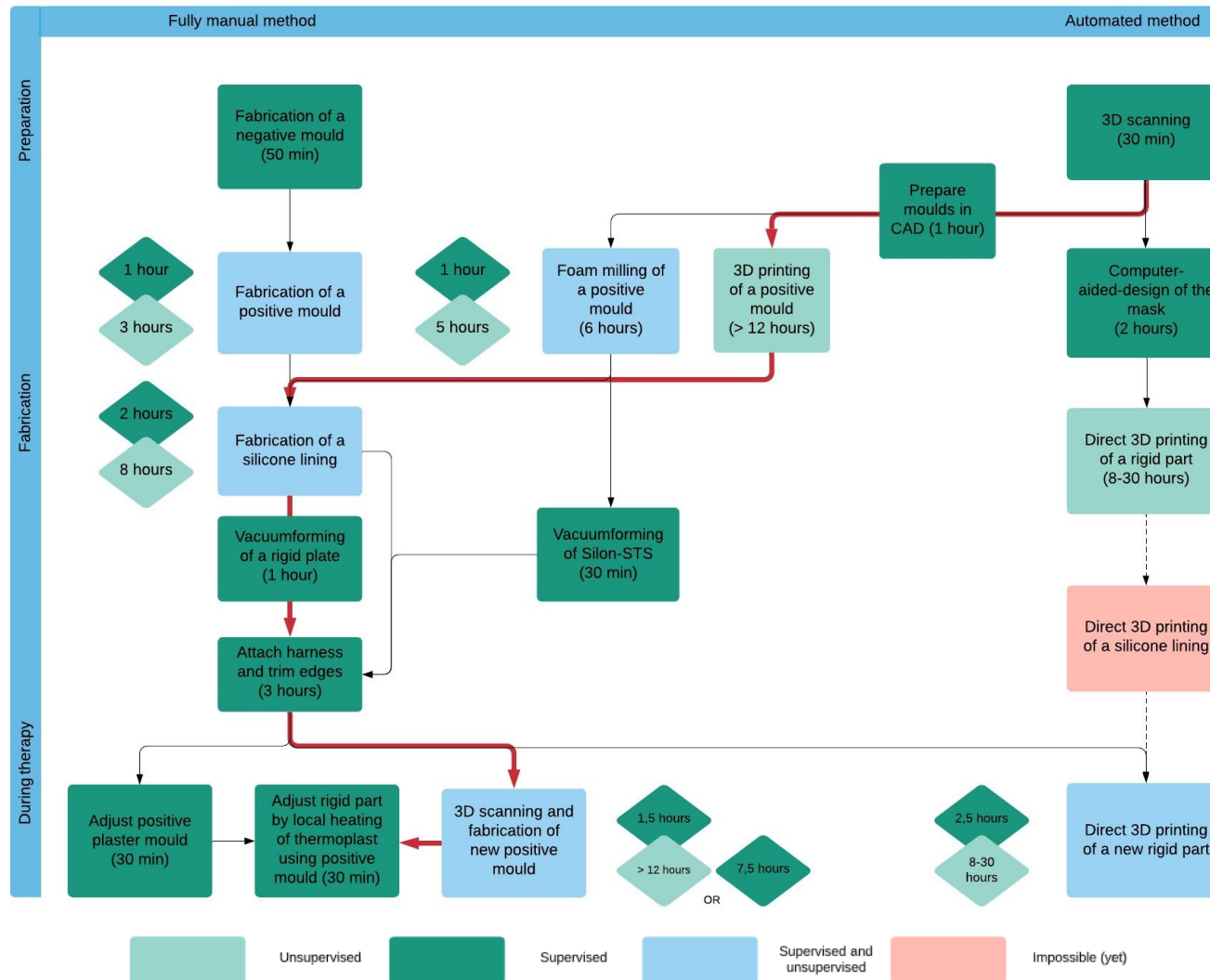
# Workflow 1



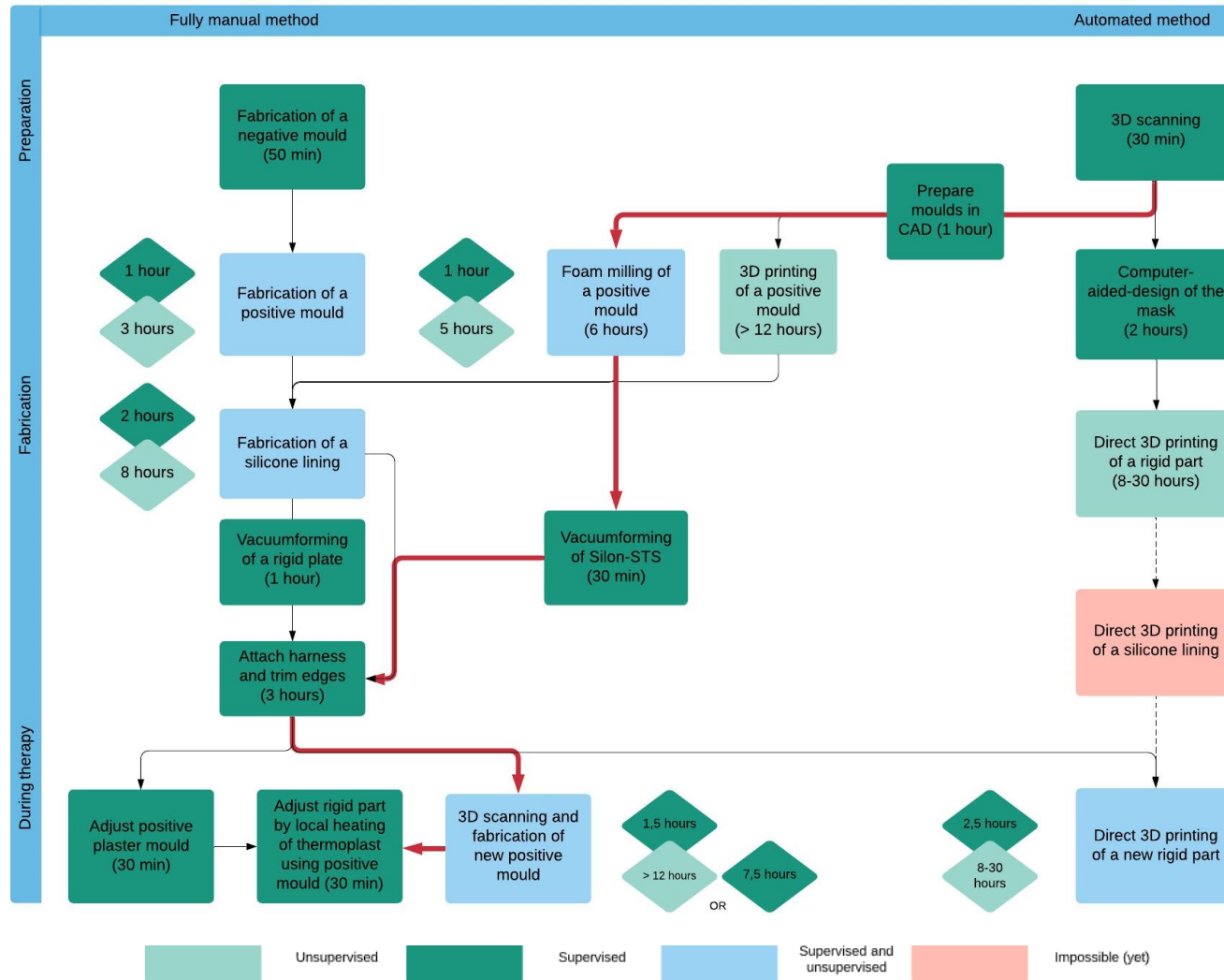
## Workflow 2



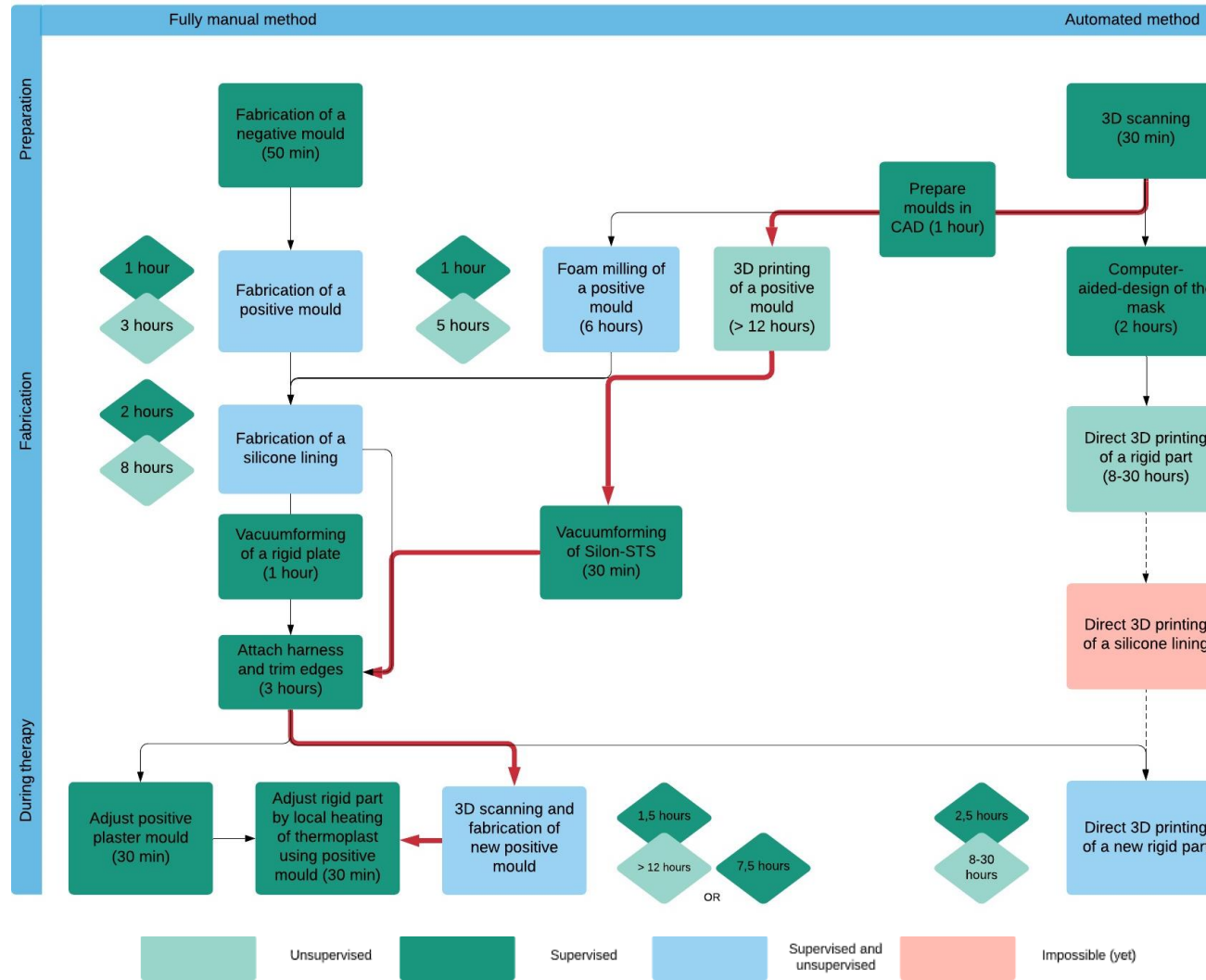
# Workflow 3



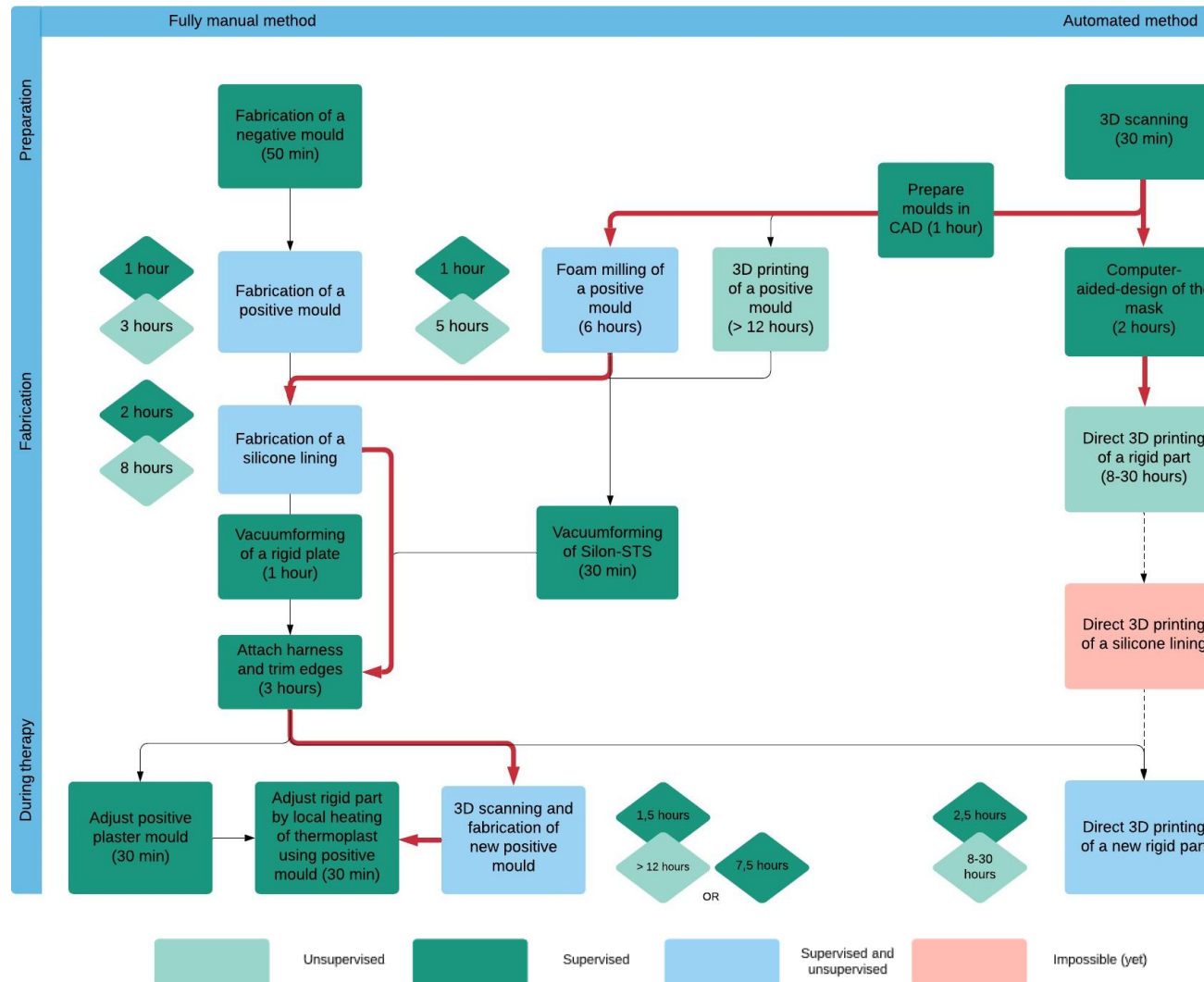
# Workflow 4



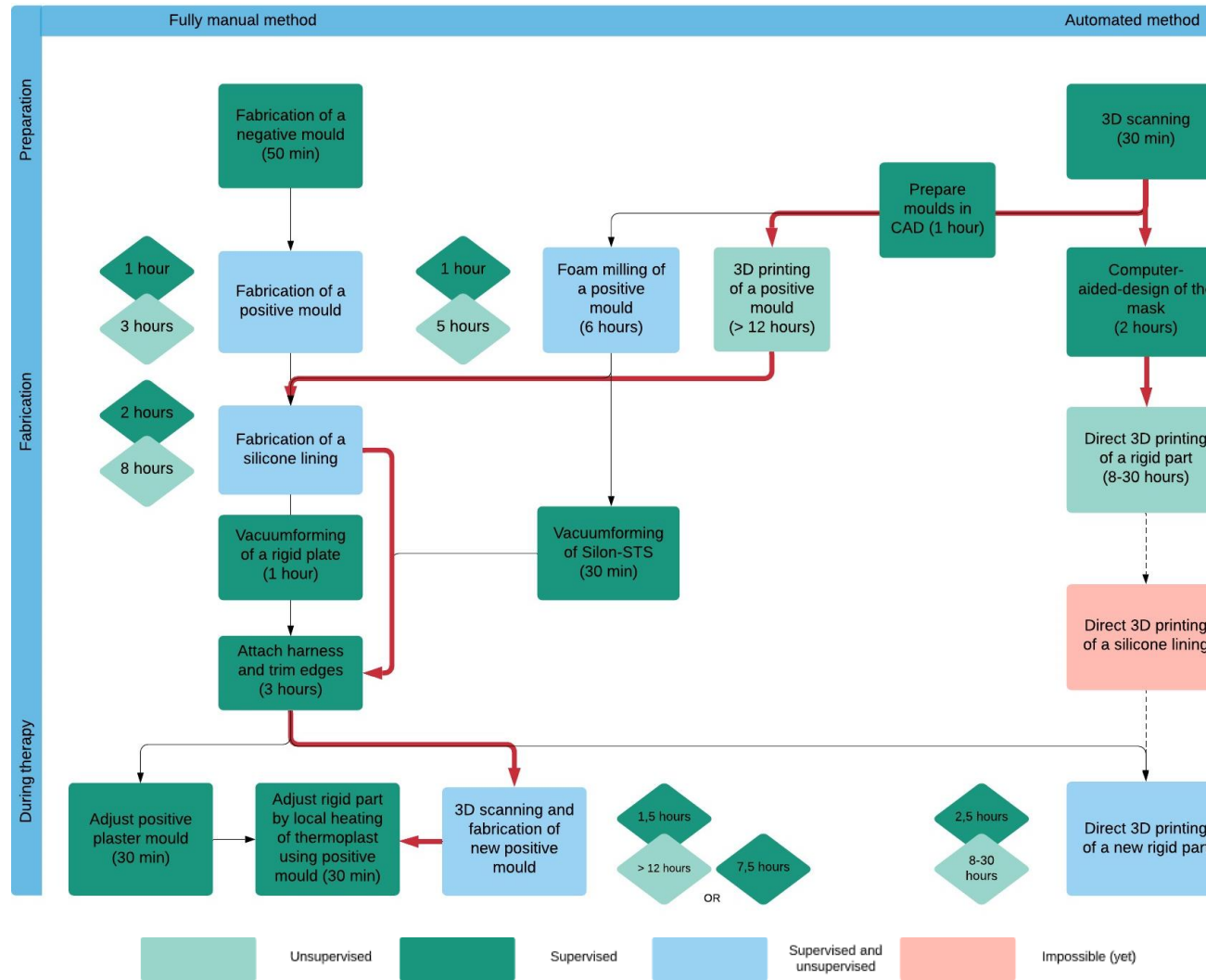
# Workflow 5



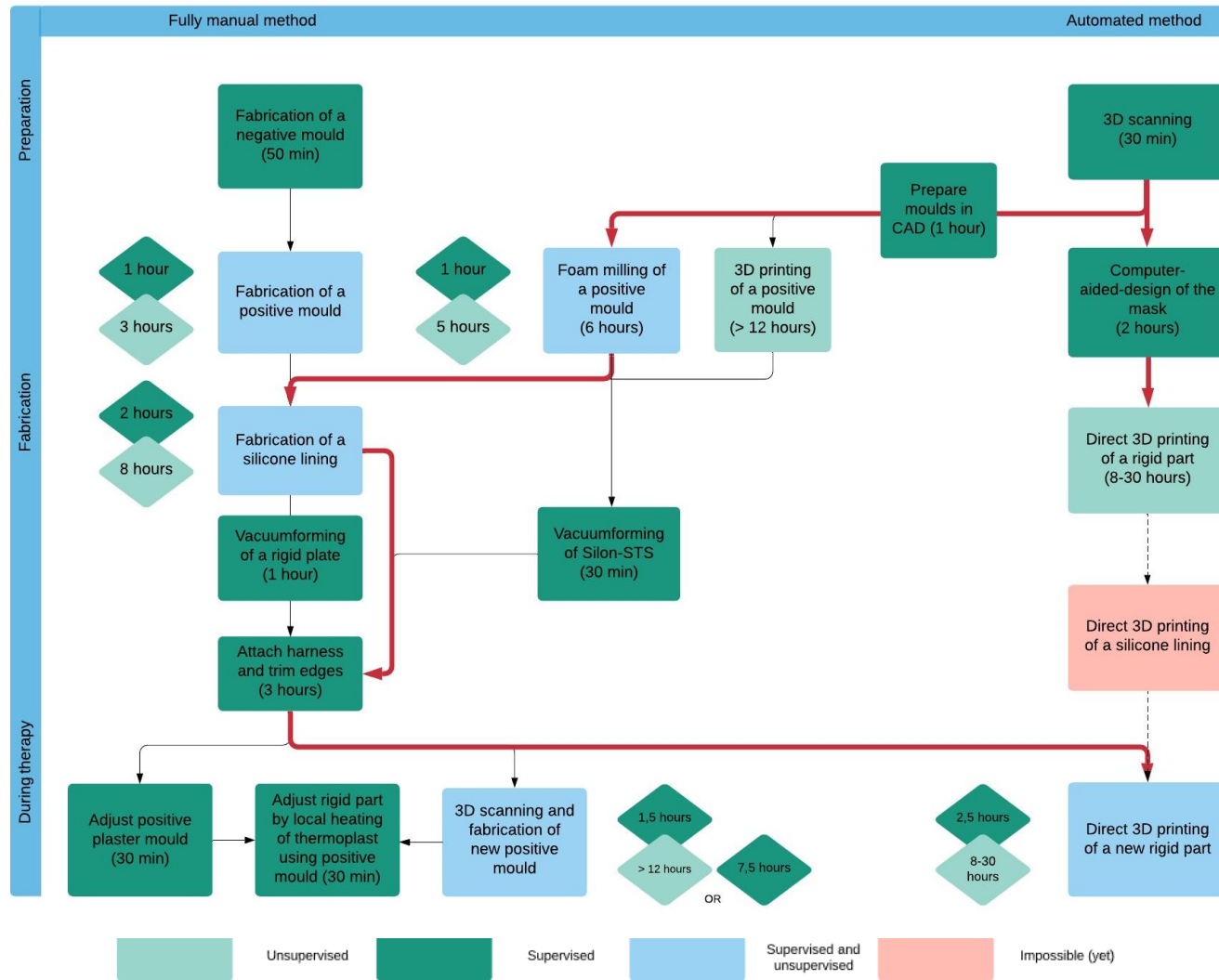
# Workflow 6



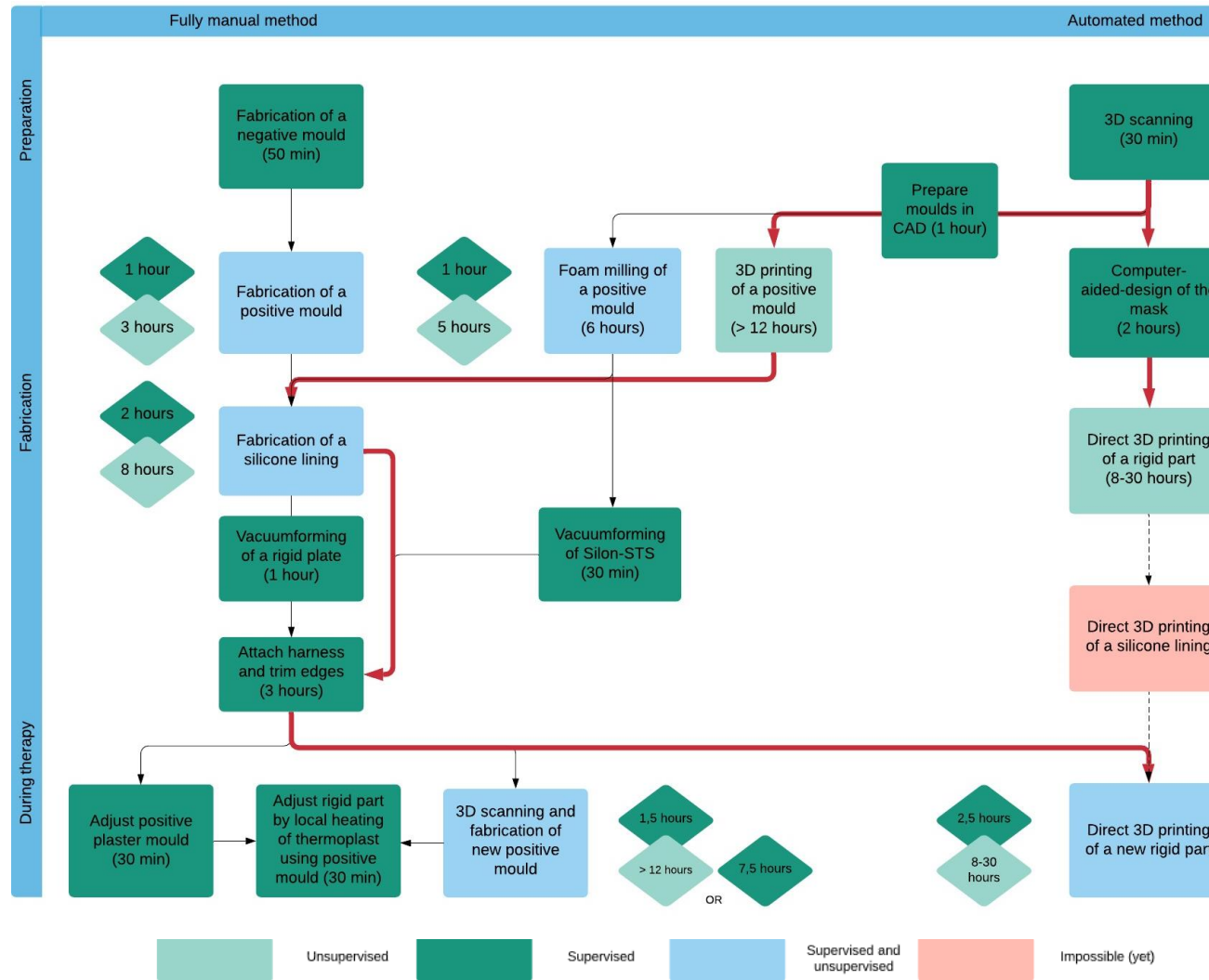
# Workflow 7



## Workflow 8



# Workflow 9



## Appendix III Literature review

### 3D printed transparent facial masks combining the effects of pressure and silicones: a literature review

BSc M.D. van Gaalen, dr. E.M.L. Corten., Prof. dr. ir. R.H.M. Goossens

#### Abstract

**Introduction:** Facial hypertrophic scarring following burn injury or surgery is a complex problem, causing both functional and psychological complaints. Two first-line non-invasive treatments of hypertrophic scars are pressure therapy and silicones. Biocompatible transparent facial pressure masks with silicone sheetings provide combined therapy, which is suggested to be more effective. Fabricating facial masks using 3D scanning and 3D printing techniques is more promising than the current (traditional) fabrication process. However, it is hypothesized that the traditionally fabricated facial mask is able to result in superior pressure distribution on the face when compared to a 3D printed facial mask. To test this hypothesis, we need to identify whether 3D printing techniques can replace the traditional fabrication method of biocompatible transparent facial pressure masks with silicone sheeting.

**Methods:** The electronic databases EMBASE, MEDLINE, Web of Science, Cochrane CENTRAL and Google Scholar were searched from 1946 to February 26th 2020 with the following combined terms: (three dimensional printing OR stereolithography OR pressure therapy OR pressure distribution OR interface pressure) AND (face OR facemask). Studies were included if (1) the 3D scanning and 3D printing techniques were used to develop a product applied to the face with or without silicone or (2) the facial pressure distribution was assessed.

**Results:** Thirty-three studies were included in this literature review. Fourteen studies investigated the use of 3D scanning and 3D printing techniques in combination with computer-aided design software to design custom-made products applied to the face. Twelve articles described the application of several tools to quantify and optimize facial pressure distribution. Seven articles were related to both 3D scanning and 3D printing techniques used to fabricate the facial masks and the assessment of facial pressure distribution. No studies showed the possibility to print biocompatible silicones directly.

**Conclusion:** This literature review shows that it is possible to fabricate biocompatible transparent facial masks that combine the effects of pressure and silicones in patients with hypertrophic scars using 3D printing techniques. However, no articles describe a technique to print the silicone masks directly. The results of this review are of informative value in the design of future studies that focus on identifying the most optimal workflow to fabricate the facial masks using 3D printing techniques.

#### Keywords

Hypertrophic scarring, Burns, Face, Transparent facial mask, 3D scanning, Computer-aided design, 3D printing, Silicones, Pressure, Pressure distribution

## Introduction

Facial hypertrophic scarring following burn injury or surgery is a complex problem, causing both functional and psychological complaints [1, 2]. Hypertrophic scars are defined as elevated scars caused by an abundant deposition of collagen at the location of injury [3].

Several non-invasive interventions are available to both prevent and treat excessive scar formation [4]. Pressure therapy is the

norm in non-invasive treatment of hypertrophic scars. It is shown that exerting mechanical pressure can lead to reduced scar thickness and scar erythema [5].

In addition to pressure therapy, silicones have become a first-line non-invasive treatment of hypertrophic scars. Silicone therapy shows positive effects on scar erythema and pliability [6]. Combined therapy is suggested to be more effective than silicone or pressure therapy alone [7, 8]. Therefore, in case of facial hypertrophic scars, biocompatible transparent facial pressure masks with silicone sheetings were developed and clinical results were positive [9] [10]. This facemask is attached to the head by a harness system with straps and anchors [11].

Currently, these masks are fabricated using plaster moulds. This method is a labour-intensive and often painful process and requires an experienced orthotist or prosthetist [12]. Recent advancements of 3D technology enable to replace the moulding process. Fabricating facemasks using 3D scanning and 3D printing could be more cost-effective and convenient than the traditional fabrication process. Furthermore, promising clinical results have been reported [13, 14].

However, Colla et al. hypothesized that the traditionally fabricated facial mask is able to result in superior pressure distribution on the face when compared to a 3D printed facemask [12]. To test this hypothesis, we need to identify whether there are studies in which 3D printing techniques replace this traditional fabrication method. Therefore, the aim of this literature review was to identify what is known about the

possibility to fabricate biocompatible transparent 3D printed facial masks that combine the effects of pressure and silicones in patients with hypertrophic scars.

Based on the results of the review, we aim to design the most optimal workflow for the 3-D printing fabrication process of these facial masks.

## Methods

### **Data sources and systematic search strategy**

A systematic literature search was performed in the databases EMBASE, MEDLINE, Web of Science, Cochrane CENTRAL and Google Scholar. The databases were searched from 1946 to February 26th 2020 with the following combined terms: (three dimensional printing OR stereolithography OR pressure therapy OR pressure distribution OR interface pressure) AND (face OR facemask). The exact search strategy is shown in Appendix I. The search was limited to studies written in English and human studies. The titles and abstracts of full text available articles were assessed on eligibility by two authors, and the relevant articles were obtained. All bibliographies of the obtained articles were screened to identify other relevant studies.

### **Study selection**

Information about both the fabrication of a 3D printed facial mask and the optimization of facial pressure distribution needs to be acquired. Therefore, studies were included if the following criteria were met: (1) 3D surface scanning and 3D printing techniques were used to develop a product applied to the face with or without silicone or (2) facial pressure distribution was assessed. The titles and abstracts of the obtained articles were screened to identify other relevant studies. Exclusion criteria were: non-living human studies, phantom studies, in vitro studies,

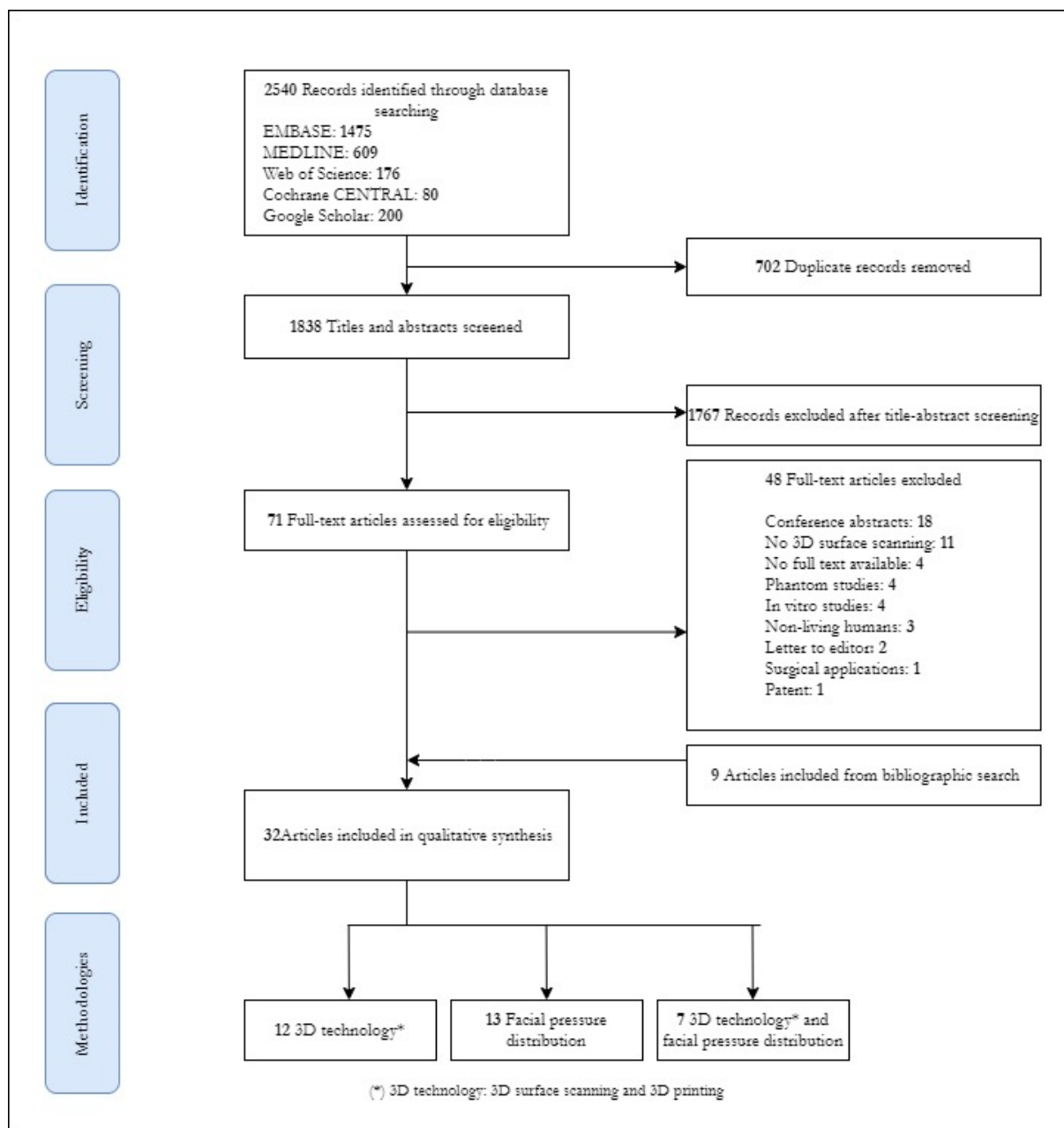


Figure 1 Flowchart according to the PRISMA guidelines

surgical applications, reviews, letter to editors, conference abstracts and patents.

### Data extraction

The following information was extracted from the included articles by one author using standardized data extraction sheets: (1) publication details (authors, year of publication); (2) study design; (3) participants (number, age); (4) type of 3D printed product; (5) 3D scan technique; (6) computer-aided design (CAD); (7) 3D print technique; (8) 3D printed material(s) (transparency,

biocompatibility); (9) use of biocompatible silicone; (10) outcome measures; (11) facial pressure distribution assessment tools.

### Quality assessment

After data inclusion and extraction, a quality assessment of the articles was carried out by two independent authors. In case of disagreement on the quality of an article, consensus was reached by discussion.

### Results

#### Study selection

The search strategy resulted in 2540 studies. After deduplication and screening on title and abstract, **71** studies were eligible for inclusion. **33** Full-text articles met the inclusion criteria and were included in this literature review (Fout! Verwijzingsbron niet gevonden.).

### Study characteristics

The included articles were published between 1984 and 2019 and a qualitative assessment was performed. The articles were categorized according to the main topics: (1) 3D printed products applied to the face and (2) facial pressure distribution. The first topic covered 12 articles, the second topic covered 13 articles and 7 articles were related to both topics. The study characteristics are shown in Table and Table 1. Specifications of 3D printing techniques and facial pressure distribution assessment tools are outlined in table 3 and 4, respectively. The main findings are given below.

### 3D printed products applied to the face

#### *Type of products*

The type of 3D printed products was classified. Five out of nineteen studies described the fabrication of facial prostheses using 3D scanning and 3D printing techniques [15-19]. Three-dimensional printed facemasks in the treatment of facial hypertrophic scarring [13, 14, 20, 21] and a radiotherapy treatment mask or bolus were the next most studied [22-25]. The fabrication of these products was investigated in four out of nineteen studies. Three out of nineteen studies focused on 3D printed fitting devices for N95 filtering facepiece respirators, non-invasive ventilation masks and pressure garments, respectively. [26-28]. Three single case studies described the use of 3D scanning and 3D printing to develop drug delivery devices, customized spectacles and respiratory protective devices [29-31].

#### *3D scanning techniques*

Thirteen out of nineteen studies investigated the use of a structured light 3D scanner\* to capture the 3D geometry of the face [13-18, 20,

25, 27-29, 31, 32]. More than 90% of these scanners were portable. Four studies described the use of (static or hand-held) 3D scanners using laser beam technology\* [19, 22, 23, 26] and three studies focused on the use of photogrammetry\* [17, 21, 30].

#### *Computer-aided design (CAD)*

All studies described the processing of a 3D scan to a digital model of the face. Several software programs were used to design a custom-made product based on the digital models. Numerous tools to mirror, align, crop and smooth objects were used and Boolean operations\* were performed. Two articles described the use of a NURBS curve\* to fit a product to a facial surface [15, 26] .

#### *3D printing techniques and materials*

Fused deposition modelling\* (FDM) was the most common 3D printing technique, investigated in eleven out of nineteen studies [18, 19, 21-29]. Five studies described the use of material jetting\* (25%) [13-17] and two studies outlined the use of stereolithography apparatus\* (SLA) [29, 30]. Two single studies described the use of selective laser sintering\* (SLS) [31] and binder jetting\* [20]. In six out of nineteen studies, biocompatible polylactic acid (PLA) was used as filament for 3D printing [18, 21, 23-25, 28]. However, no studies described the use of transparent PLA. The next most used biocompatible materials were acrylonitrile butadiene styrene (ABS) [19, 26] and transparent PolyJet material [13, 14], both described in two studies. The use of biocompatible semi-transparent NinjaFlex (NF), transparent Flex EcoPLA (FPLA) [29] and thermoplastic polyurethane (TPU) [31] was outlined in two single case studies.

#### *Biocompatible transparent silicone*

Five studies described the use of biocompatible silicone to develop facial prostheses [16, 18, 19] and fitting devices [27, 28]. In all cases, a mould was 3D printed and silicone was poured into a mould. Two of these biocompatible silicones were transparent [16, 19]. Unkovskiy et al. [17]

investigated direct 3D printing of a silicone prosthesis that was only suitable as interim post-surgical appliance as the silicone was not biocompatible. Two studies investigating the fabrication method of a 3D printed facial pressure mask for patients with hypertrophic scars described the additional use of transparent medical silicone gel as part of the treatment. [13, 14].

## Facial pressure distribution

### *Type of products*

Two-thirds of the studies investigated facial pressure distribution applied by a product that was specifically developed to apply pressure to the face. These products included facial pressure masks with or without silicone lining [11-14, 20, 21, 33-37] and pressure garments [28, 38]. Other studies assessed facial pressure distribution applied by N95 filtering facepieces [26, 39, 40] and non-invasive ventilation masks [27, 41, 42]. A single randomized controlled trial assessed pressure applied to the face by a force controlled algometer\* [43]. *Outcome measures*

Sixteen out of twenty articles assessed interface pressure or pressure distribution directly [11, 12, 14, 20, 26-28, 33, 34, 37-41, 43, 44]. Seven articles investigated the (indirect) effects of the applied pressure by quantifying skin perfusion [35, 36], blanching of skin erythema [5, 27], temperature and humidity [35, 41] and comfort [11, 27, 41, 44].

### *Direct assessment of facial pressure (distribution)*

Most studies described the use of pressure sensors to quantify pressure distribution (Pa/cm<sup>2</sup>) or interface pressure in Pascal (Pa) or millimetres of mercury (mmHg) [12, 14, 26-28, 34, 37, 38, 41, 43, 44]. Four out of five articles that described the use of sensors to quantify pressure in case of facial pressure therapy outlined a minimum required pressure, which ranged from 10 mmHg in case of poor tolerance

to 25 mmHg [10, 12, 14, 38]. Two articles outlined that the applied pressure should not exceed 40 mmHg, which is assumed to be the threshold of pressure ulcer formation [27, 28]. The chin, cheek, forehead and nasal bridge are the most common locations [14, 26-28, 34, 38, 41, 43]. Three articles about transparent facial pressure masks assessed interface pressure by visually checking appropriate blanching of scars [12, 20, 33]. Shikama et al. [27] investigated the use of a stretchable strain sensor to quantify tension on the head straps of non-invasive ventilation masks.

### *Indirect assessment of facial pressure (distribution)*

A scanning laser Doppler technique was used to quantify skin perfusion, one of the (indirect) effects of the applied pressure [35, 36]. Skin temperature and humidity at the mask-skin interface were quantified using a combined sensor able to measure both temperature (°C) and relative humidity (% RH) [41, 44]. Blanching of skin erythema was quantified by Shikama et al. [27]. The maximum Erythema Index with and without a fitting device was calculated using ImageJ software (National Institutes of Health) as described by Yamamoto et al. [45]. Three articles assessed comfort by a 10-point visual analogue scale (VAS) [27, 41, 44].

### *Optimal facial pressure distribution*

In all articles, optimal facial pressure distribution is defined as an overall constant pressure applied to the face. In case of facial pressure therapy, this means that pressure should be released on bony prominences and more pressure should be exerted on soft tissue. Furthermore, additional pressure should be applied at the scarred area. The development of a finite element model\* (FEM) that can be used to generate the most optimal facial pressure distribution was introduced in three articles [13, 14, 40].

Three-dimensional scanning techniques were investigated as tools to assess pressure distribution by aligning CAD models of scans

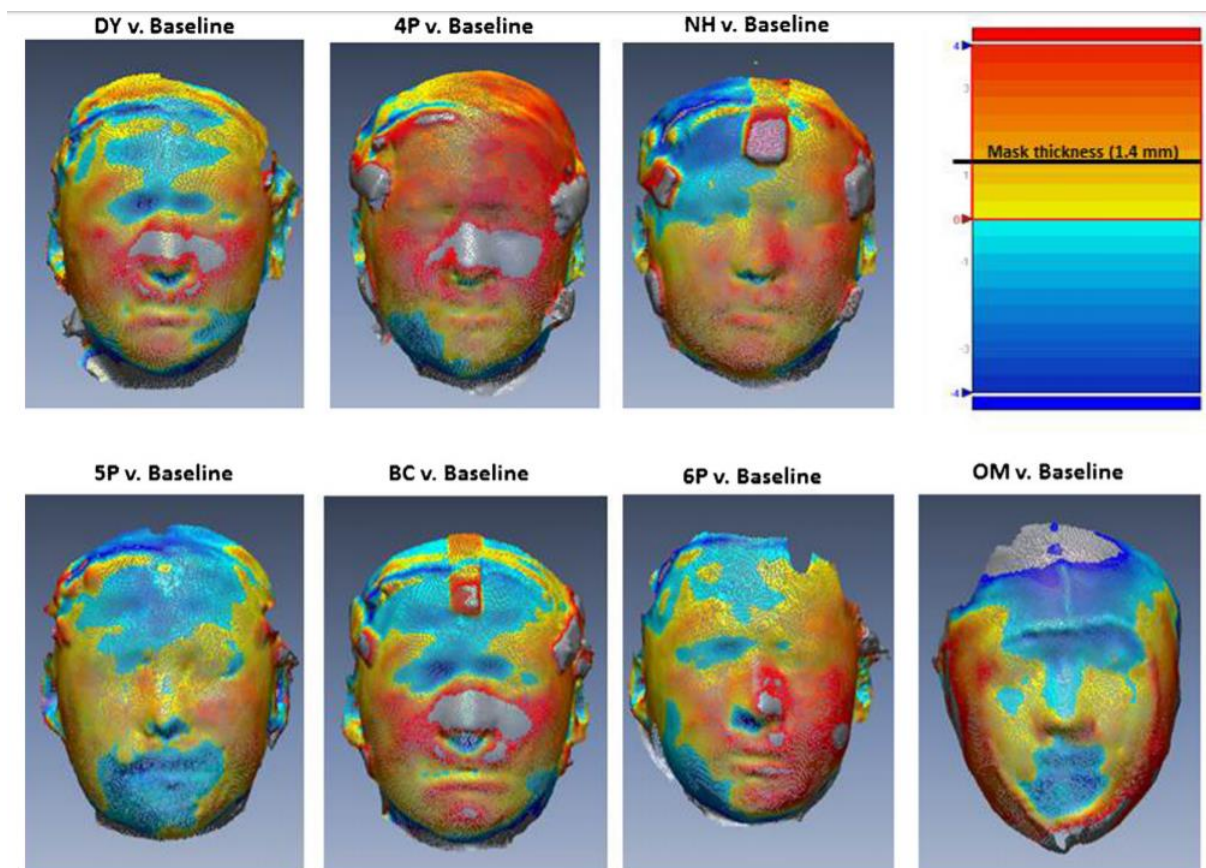


Figure 2 Surface pressure mapping: scanned images without mask aligned with scanned images with mask. The thickness of the mask itself is marked at 1.4 mm (dark yellow). Orange and red areas signify no compression, whereas yellow and blue areas signify compression.

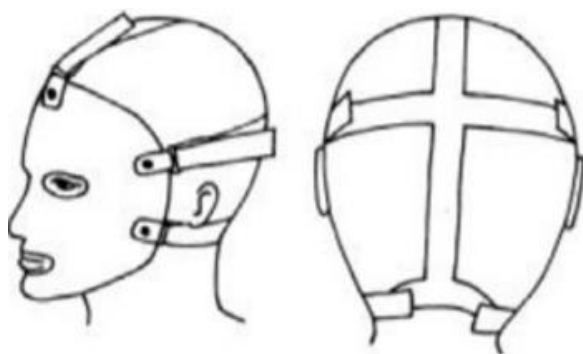


Figure 3 Five-point harness design as described by Parry et al.

with and without facial masks and creating colour map deviations\* [11, 39]. Parry et al. [11] made a comparison between the colour map deviations of different harness designs for facial pressure therapy (Figure ). The images lend support to a 5-point harness design for an even pressure distribution throughout the face (Figure ) [11].

## Discussion

### Major findings

This literature review provides an overview of suitable techniques and assessment tools that can be used to fabricate biocompatible transparent facial masks that combine the effects of pressure and silicones in patients with hypertrophic scars using 3D printing techniques.

Although several 3D scanning techniques were investigated and all techniques appeared suitable to capture the 3D geometry of the face, most studies described the use of a (hand-held) structured light 3D scanner. Therefore, this technique is likely to be an appropriate technique for this purpose. However, the most suitable 3D scanning technique cannot be distinguished based on the results of this review due to the low quality of the included articles.

Furthermore, computer-aided-design software that includes the tools to create a NURBS curve used to fit a mask to a facial surface could be of added value in the fabrication of the facial mask using 3D printing techniques [15, 26].

No studies showed the possibility to 3D print biocompatible silicone facial masks directly. Based on the results of this review, the most optimal workflow to fabricate the facial masks should contain the fabrication of a 3D printed mould for silicone pouring. The fabricated silicone sheeting could be attached to a 3D printed (transparent) facial mask, as several 3D printing techniques and biocompatible transparent materials for 3D printing have successfully been used for developing custom-made products applied to the face. Most studies investigated FDM and the use of biocompatible PLA. Therefore, it is assumed that FDM and the use of PLA could be included in a workflow to fabricate facial masks using 3D printing techniques. However, the most suitable 3D printing techniques and materials cannot be distinguished based on the results of this literature review due to the low quality of the included articles.

Some studies integrated the use of facial pressure distribution assessment tools in a 3D printing fabrication process of a product applied to the face. The development of a finite element model (FEM) and the use of 3D scanning techniques to create colour map deviations could be of added value in designing the most optimal workflow to fabricate the silicone facial masks. For example, Parry et al. [11] used colour map deviations to show that a 5-point harness design provides an even pressure distribution.

Pressure sensors can be used to quantify facial pressure distribution applied by the fabricated silicone facial mask. As the sensors must be placed between the mask and the face, thin sensors are required. In three articles, the use of thin sensors was highlighted [14, 27, 43]. The effects of applied pressure can be assessed indirectly as well by quantifying (1) skin perfusion, (2) skin temperature and humidity, (3) comfort and (4) blanching of skin erythema. Laser Doppler [35], temperature sensors [41], a 10-point VAS score [27] and free ImageJ software [45] appeared suitable tools to quantify these effects, respectively. In theory, all tools mentioned above are complementary to each other in the evaluation of the (indirect) effects of the applied pressure. However, high-

quality articles considering the optimal tools are lacking. Practical considerations such as availability of devices, costs and technical feasibility should be taken into account.

### **Previous research**

To our knowledge, this is the first systematic review that studied the fabrication of transparent facial masks that combine the effects of pressure and silicones in patients with hypertrophic scarring using 3D printing techniques. Moreover, facial pressure distribution is investigated explicitly. Previous reviews focused on medical applications of 3D scanning and 3D printing and the clinical effects of transparent facial pressure masks, respectively [46-48]. A review on silicone additive manufacturing conducted by Liravi et al. showed that further research must be carried out on the development of suitable 3D printing techniques and materials for directly printing biocompatible silicones [49]. This is in line with our finding that no studies showed that direct 3D printing of biocompatible silicones is possible.

### **Strengths and limitations**

The major strength of this literature review is that it was performed in a systematic way. This makes it unlikely that articles were missed that should be included. However, based on 18 excluded conference abstracts, it is likely that more technical knowledge is already available on this subject, although not published in peer-reviewed articles.

Several remarks can be made about this literature review. Only studies that investigated both 3D scanning and 3D printing techniques were included. Therefore, studies describing the fabrication process of a 3D printed product applied to the face using other imaging modalities (CT, MRI) to capture the 3D geometry of the face were excluded. Moreover, the use of milling machines fell outside the scope of this review, as this review was limited to 3D printing techniques. Rogers et al. successfully investigated a fabrication process using 3D scanning, milling and vacuum forming [50]. This process could be an appropriate

alternative to 3D printing and should be further researched.

Another remark is the low quality of the included studies. Almost 75% of the included studies are case studies or series, feasibility studies and pilot studies. Furthermore, few specifications of the investigated techniques and assessment tools were provided by the authors of the included studies.

### Clinical impact and future research

Based on the results of this review, we aim to design the most optimal workflow to fabricate facial masks that combine the effects of pressure and silicones using 3D printing techniques. This literature review provides an overview of suitable techniques and assessment tools that can be used to fabricate these masks. This overview is of informative value in the design of future studies. Further research should include a thorough analysis of the investigated suitable techniques and assessment tools to define the most optimal workflow. Thereafter, future studies should investigate whether 3D printed facial masks can provide adequate facial pressure therapy in patients with hypertrophic scarring. Other important future goals are to compare cost-effectiveness and long-term clinical effects for both the traditional and 3D printing fabrication processes.

### Conclusion

This literature review provides an overview of what is known about the possibilities to fabricate biocompatible transparent facial masks that combine the effects of pressure and silicones in patients with hypertrophic scarring using 3D printing techniques. No articles describe a technique to 3D print the silicone facial masks directly. However, several other suitable techniques and assessment tools that can be used to fabricate these masks were outlined. The results of this review are of informative value in the design of future studies that focuses on identifying the most optimal

workflow to fabricate the silicone facial pressure masks using 3D printing techniques.

### Acknowledgements

The authors wish to thank W.M. Bramer from the Erasmus MC Medical Library for the assistance in developing the search strategies.

### References

1. Bock, O., et al., *Quality of life of patients with keloid and hypertrophic scarring*. Arch Dermatol Res, 2006. **297**(10): p. 433-8.
2. Gibson, J.A.G., et al., *The association of affective disorders and facial scarring: Systematic review and meta-analysis*. J Affect Disord, 2018. **239**: p. 1-10.
3. Gauglitz, G.G., et al., *Hypertrophic scarring and keloids: pathomechanisms and current and emerging treatment strategies*. Mol Med, 2011. **17**(1-2): p. 113-25.
4. Anthonissen, M., et al., *The effects of conservative treatments on burn scars: A systematic review*. Burns, 2016. **42**(3): p. 508-18.
5. Van den Kerckhove, E., et al., *The assessment of erythema and thickness on burn related scars during pressure garment therapy as a preventive measure for hypertrophic scarring*. Burns, 2005. **31**(6): p. 696-702.
6. Van den Kerckhove, E., et al., *Silicones in the rehabilitation of burns: a review and overview*. Burns, 2001. **27**(3): p. 205-14.
7. Steinstraesser, L., et al., *Pressure garment therapy alone and in combination with silicone for the prevention of hypertrophic scarring: randomized controlled trial with intraindividual comparison*. Plast Reconstr Surg, 2011. **128**(4): p. 306e-313e.
8. Li-Tsang, C.W., Y.P. Zheng, and J.C. Lau, *A randomized clinical trial to study the effect of silicone gel dressing and pressure therapy on posttraumatic hypertrophic scars*. J Burn Care Res, 2010. **31**(3): p. 448-57.
9. Rivers, E.A., R.G. Strate, and L.D. Solem, *The transparent face mask*. Am J Occup Ther, 1979. **33**(2): p. 108-13.
10. Kant, S.B., et al., *A new treatment for reliable functional and esthetic outcome after local facial flap reconstruction: a transparent polycarbonate facial mask with silicone sheeting*. Eur J Plast Surg, 2017. **40**(5): p. 407-416.

11. Parry, I., et al., *Harnessing the Transparent Face Orthosis for facial scar management: a comparison of methods*. Burns, 2013. **39**(5): p. 950-6.
12. Colla, C., et al., *Manual fabrication of a specialized transparent facial pressure mask: A technical note*. Prosthet Orthot Int, 2019. **43**(3): p. 356-360.
13. Wei, Y., et al., *3D-printed transparent facemasks in the treatment of facial hypertrophic scars of young children with burns*. Burns, 2017. **43**(3): p. e19-e26.
14. Wei, Y., et al., *The application of 3D-printed transparent facemask for facial scar management and its biomechanical rationale*. Burns, 2018. **44**(2): p. 453-461.
15. Bockey, S., et al., *Computer-aided design of facial prostheses by means of 3D-data acquisition and following symmetry analysis*. J Cranio-Maxillofac Surg, 2018. **46**(8): p. 1320-1328.
16. Fan, S., et al., *Personalised anaesthesia: three-dimensional printing of facial prosthetic for facial deformity with difficult airway*. Br J Anaesth, 2018. **121**(3): p. 675-678.
17. Unkovskiy, A., et al., *Direct 3D printing of silicone facial prostheses: A preliminary experience in digital workflow*. J Prosthet Dent, 2018. **120**(2): p. 303-308.
18. Cevik, P. and M. Kocacikli, *Three-dimensional printing technologies in the fabrication of maxillofacial prosthesis: A case report*. Int J Artif Organs, 2019.
19. De Crescenzo, F., et al., *Design and manufacturing of ear prosthesis by means of rapid prototyping technology*. Proc Inst Mech Eng H, 2011. **225**(3): p. 296-302.
20. Pilley, M.J., et al., *The use of non-contact structured light scanning in burns pressure splint construction*. Burns, 2011. **37**(7): p. 1168-1173.
21. guilar, H.A. and H.F. Mayer, *A New Method for Securing Dermal Substitutes and Skin Grafts to Difficult Portions of the Face Using a Custom 3D-Printed Facemask*. J Burn Care Res, 2019. **40**(6): p. 1015-1018.
22. Briggs, M., et al., *3D printed facial laser scans for the production of localised radiotherapy treatment masks - A case study*. J Vis Commun Med, 2016. **39**(3-4): p. 99-104.
23. Dipasquale, G., et al., *Improving 3D-printing of megavoltage X-rays radiotherapy bolus with surface-scanner*. Radiat Oncol, 2018. **13**(1).
24. Sharma, A., et al., *Low-cost optical scanner and 3-dimensional printing technology to create lead shielding for radiation therapy of facial skin cancer: First clinical case series*. Adv Radiat Oncol, 2018. **3**(3): p. 288-296.
25. LeCompte, M.C., et al., *Simple and Rapid Creation of Customized 3-dimensional Printed Bolus Using iPhone X True Depth Camera*. Pract Radiat Oncol, 2019. **9**(4): p. e417-e421.
26. Cai, M., et al., *Customized design and 3D printing of face seal for an N95 filtering facepiece respirator*. J Occup Environ Hyg, 2018. **15**(3): p. 226-234.
27. Shikama, M., et al., *Development of personalized fitting device with 3-dimensional solution for prevention of niv oronasal mask-related pressure ulcers*. Respir Care, 2018. **63**(8): p. 1024-1032.
28. ozi, M.A.A., M.N. Salleh, and K.A. Ismail, *Development of 3D-printed customized facial padding for burn patients*. Rapid Prototyping J., 2019. **25**(1): p. 55-61.
29. Goyanes, A., et al., *3D scanning and 3D printing as innovative technologies for fabricating personalized topical drug delivery systems*. J Control Release, 2016. **234**: p. 41-48.
30. Ayyildiz, O., *Customised spectacles using 3-D printing technology*. Clin Exp Optom, 2018. **101**(6): p. 747-751.
31. Makowski, K. and M. Okrasa, *Application of 3D scanning and 3D printing for designing and fabricating customized half-mask facepieces: A pilot study*. WORK, 2019. **63**(1): p. 125-135.
32. Sharma, A., et al., *Using optical scanner and 3d printer technology to create lead shielding for radiotherapy of facial skin cancer with low energy photons: An exciting innovation*. Radiother Oncol, 2016. **120**: p. S33-S34.
33. Powell, B.W., C. Haylock, and J.A. Clarke, *A semi-rigid transparent face mask in the treatment of postburn hypertrophic scars*. Br J Plast Surg, 1985. **38**(4): p. 561-6.
34. Groce, A., et al., *Are your thoughts of facial pressure transparent? J Burn Care Rehabil*, 1999. **20**(6): p. 478-81.
35. Allely, R.R., et al., *Laser doppler imaging of cutaneous blood flow through transparent face masks: A necessary preamble to computer-controlled rapid prototyping fabrication with submillimeter precision*. J Burn Care Res, 2008. **29**(1): p. 42-48.

36. Van-Buendia, L.B., et al., *What's behind the mask? A look at blood flow changes with prolonged facial pressure and expression using laser doppler imaging.* J Burn Care Res, 2010. **31**(3): p. 441-447.
37. Kant, S.B., et al., *A new treatment for reliable functional and esthetic outcome after local facial flap reconstruction: a transparent polycarbonate facial mask with silicone sheeting.* Eur J Plast Surg, 2017. **40**(5): p. 407-416.
38. Cheng, J.C.Y., et al., *Pressure therapy in the treatment of post-burn hypertrophic scar—a critical look into its usefulness and fallacies by pressure monitoring.* Burns, 1984.
39. Niezgoda, G., et al., *Flat Fold and Cup-Shaped N95 Filtering Facepiece Respirator Face Seal Area and Pressure Determinations: A Stereophotogrammetry Study.* Journal of Occupational and Environmental Hygiene, 2013. **10**(8): p. 419-424.
40. Cai, M., et al., *Study of contact characteristics between a respirator and a headform.* Journal of occupational and environmental hygiene, 2016. **13**(3): p. D50-D60.
41. Worsley, P.R., et al., *Investigating the effects of strap tension during non-invasive ventilation mask application: A combined biomechanical and biomarker approach.* Med Devices Evid Res, 2016. **9**: p. 409-417.
42. Alqahtani, J., P. Worsley, and D. Voegeli, *The additive effect of humidification with noninvasive ventilation (NIV) in the development of interface facial pressure ulcers: An experimental study.* Chest, 2017. **152**(4): p. A185.
43. Melia, M., et al., *Pressure pain thresholds: Subject factors and the meaning of peak pressures.* Eur J Pain, 2019. **23**(1): p. 167-182.
44. Alqahtani, J., P. Worsley, and D. Voegeli, *Effects of noninvasive ventilation (NIV) settings on facial skin interface pressures: An exploratory study.* Eur Respir J, 2017. **50**.
45. Yamamoto, T., et al., *Derivation and clinical application of special imaging by means of digital cameras and Image J freeware for quantification of erythema and pigmentation.* Skin Res Technol, 2008. **14**(1): p. 26-34.
46. Haleem, A. and M. Javaid, *3D scanning applications in medical field: A literature-based review.* Clinical Epidemiology and Global Health, 2019. **7**(2): p. 199-210.
47. Ventola, C.L., *Medical Applications for 3D Printing: Current and Projected Uses.* P & T : a peer-reviewed journal for formulary management, 2014. **39**(10): p. 704-711.
48. Kant, S.B., et al., *Clinical effects of transparent facial pressure masks: A literature review.* Prosthet Orthot Int, 2019. **43**(3): p. 349-355.
49. Liravi, F. and E. Toyserkani, *Additive manufacturing of silicone structures: A review and prospective.* Additive Manufacturing, 2018. **24**: p. 232-242.
50. Rogers, B., et al., *Computerized manufacturing of transparent face masks for the treatment of facial scarring.* 2003. **24**(2): p. 91-96.

## Appendix I – Literature search

### **Embase.com (1971-) 1475**

('three dimensional printing'/de OR 'stereolithography'/de OR 'pressure therapy'/de OR 'interface pressure'/de OR (((three-dimensional OR 3-dimensional OR 3d OR 3-d) NEAR/3 (print\*)) OR stereolithograph\* OR stereo-lithograph\* OR (pressure NEAR/3 (therap\* OR distribution\* OR interface\*)) OR (strap\* NEAR/3 tension\*)):ab,ti) AND ('face'/exp OR 'face mask'/de OR cephalometry/de OR 'face malformation'/exp OR 'facies'/de OR 'face tumor'/exp OR 'face scar'/de OR 'face injury'/exp OR (face OR midface OR forehead OR facemask\* OR facial OR mask OR masks OR eyelid\* OR chin OR cephalometr\* OR maxillofac\* OR facies):ab,ti) NOT ((animal/exp OR animal\*:de OR nonhuman/de) NOT ('human'/exp)) AND [English]/lim NOT ('positive end expiratory pressure'/mj OR (cpap OR pap OR Positive-Airway-Pressure OR (Negative-pressure NEAR/3 therap\*)):ti)

### **Medline ALL Ovid (1946-) 609**

(exp Printing, Three-Dimensional/ OR (((three-dimensional OR 3-dimensional OR 3d OR 3-d) ADJ3 (print\*)) OR stereolithograph\* OR stereo-lithograph\*).ab,ti.) AND (Face/ OR Masks/ OR Cephalometry/ OR face malformation/ OR Facies/ OR exp Facial Neoplasms/ OR face scar/ OR Facial Injuries/ OR (face OR midface OR forehead OR facemask\* OR facial OR mask OR masks OR eyelid\* OR chin OR cephalometr\* OR maxillofac\* OR facies).ab,ti.) NOT ((exp animal/) NOT (human/)) AND english.la.

### **Web of science Core Collection (1975-) 176**

TI=((((three-dimensional OR "3-dimensional" OR 3d OR "3-d") NEAR/2 (print\*)) OR stereolithograph\* OR stereo-lithograph\* OR (pressure NEAR/2 (therap\* OR distribution\* OR interface\*)) OR (strap\* NEAR/2 tension\*))) AND ((face OR midface OR forehead OR facemask\* OR facial OR mask OR masks OR eyelid\* OR chin OR cephalometr\* OR maxillofac\* OR facies))) NOT TI=((cpap OR pap OR Positive-Airway-Pressure OR (Negative-pressure NEAR/2 therap\*)))

### **Cochrane CENTRAL register of trials (1992-) 80**

(((((three-dimensional OR "3-dimensional" OR 3d OR "3-d") NEAR/3 (print\*)) OR stereolithograph\* OR stereo-lithograph\* OR (pressure NEAR/3 (therap\* OR distribution\* OR interface\*)) OR (strap\* NEAR/3 tension\*)):ab,ti) AND ((face OR midface OR forehead OR facemask\* OR facial OR mask OR masks OR eyelid\* OR chin OR cephalometr\* OR maxillofac\* OR facies):ab,ti) NOT ((cpap OR pap OR Positive-Airway-Pressure OR (Negative-pressure NEAR/3 therap\*)):ti)

### **Google scholar**

"three|3 dimensional|d printing|"3d printing"|stereolithography|"pressure therapy|distribution" face|midface|forehead|facemask|facial|mask|cephalometry

## Appendix II – Glossary

### **3D scanning**

Laser beam technology	A scanning technique that projects a laser beam onto the object and captures the reflected light. The surface shape depends on the time of flight of the laser beam that increases with the distance between the sending device and the object.
Photogrammetry	A scanning technique based on (multiple) photographs.
Structured light scanning	A scanning technique that projects light onto the object and captures the deformed light pattern by cameras.

### **Computer-aided design (CAD)**

Boolean operations	Functionality in 3D modeling to fuse or subtract objects.
NURBS curve	Non-uniform Rational B-Splines: mathematical model used for generating and representing curves and surfaces.

### **3D printing**

Binder jetting	A liquid binder agent is deposited onto a powder bed, bonding the powder together to form a solid part.
Fused deposition modeling (FDM)	Layer-by-layer deposition of a thermoplastic filament by a moving heated extruder head (nozzle).
Material jetting	Deposition of droplets of a photosensitive material on a building platform. After each layer, UV light activates the curing process.
Selective laser sintering (SLS)	A high power laser is used to fuse small particles of metal, plastic, ceramic or glass powder.
Stereolithography apparatus (SLA)	Light-sensitive resins (liquid materials) are turned into solid 3D objects by shining a ultraviolet laser on it.

### **Facial pressure distribution**

Algometer	Measures the amount of pressure required to evoke a painful response.
Color map deviations	Tool to map distances between (and indirectly compression on) objects. For example, orange and red signify a positive distance and therefore no compression. Yellow and blue signify a negative distance and therefore compression.
Finite element modeling	A computational technique that can be used to simulate and assess the biomechanics of the musculoskeletal system, including soft tissue mechanics.
10-point Visual Analog Scale	An instrument used to measure the intensity or frequency of symptoms. The scale ranges from 0 to 10, where 0 represents no symptoms and 10 extreme symptoms

## Tables

Table 1 Study characteristics 3D printed products applied to the face

Authors (year of publication)	Study design	Product	Number of participants (male)	Mean age (range)
De Crescenzo et al. (2011)	Case study	Ear prosthesis	1 patient (1)	NS (NA)
Briggs et al. (2016)	Case study	Radiotherapy treatment mask	1 patient (1)	NS (NA)
Goyanes et al. (2016)	Feasibility study	Drug delivery device	1 patient (0)	NS (NA)
Ayyildiz. (2018)	Feasibility study	Customized spectacles	1 patient (0)	5 (NA)
Bockey et al. (2018)	Case series	Facial prosthesis	32 patients (18)	NS (46-87)
Dipasquale et al. (2018)	Feasibility study	Radiotherapy bolus	10 volunteers (6)	NS (23-60)
Fan S et al. (2018)	Case study	Facial prosthesis for facial deformity with difficult airway	1 patient (0)	73 (NA)
Sharma et al. (2018)	Case series	Lead shielding for radiation therapy	10 patients (3)	76 (62-85)
Unkovskiy et al. (2018)	Case study	Nasal prosthesis	1 patient (0)	40 (NA)
Cevik et al. (2019)	Case study	Ear prosthesis	1 patient (1)	24 (NA)
LeCompte et al. (2019)	Feasibility study	Radiotherapy bolus	7 patients (NS)	NS (NS)
Makowski et al. (2019)	Pilot study	Respiratory Protective Devices (RPD)	1 volunteer (1)	33 (NA)
Pilley et al. (2011)	Case study	Face mask	1 patient (0)	9 (NA)
Wei et al. (2017)	Case series	Face mask	2 patients (2)	3.5 (1-6)
Cai et al. (2018)	Case series	N95 FFR face seal	3 volunteers (NS)	NS (NS)
Shikama et al. (2018)	RCT	Fitting device for NIV oronasal mask	20 volunteers (3)	NS (NS)
Wei et al. (2018)	Pilot study	Face mask	10 patients (7)	31.5 (14-50)
Ozi et al. (2019)	Feasibility study	Facial padding	1 patient (1)	NS (NS)
Guilar et al. (2019)	Case study	Face mask for securing dermal substitutes and skin grafts and pressure therapy	1 patient (1)	38 (NA)

Abbreviations: NA - not applicable; NS - not specified

Table 1 Study characteristics facial pressure distribution

Authors (year of publication)	Study design	Product	Number of participants (male)	Mean age (range)
Cheng et al. (1984)	Case series	Pressure garments	60 patients	NS (NS)
Powell et al. (1985)	Case series	Transparent face mask	4 patients (2)	12 (0-38)
Groce et al. (1999)	Comparative study	Transparent face mask	1 volunteer (0)	NS (NS)
Allely et al. (2008)	Feasibility study	Transparent face mask (with silicone lining)	5 volunteers (1)	NS (28-55)
Van-Buendia et al. (2010)	Case series	Transparent plastic face masks	6 patients (1)	35 (26-42)
Niezgoda et al. (2013)	Feasibility study	N95 filtering facepiece	20 volunteers (13)	23 (NS)
Parry et al. (2013)	Comparative study	Transparent face orthosis	1 patient (0)	10 (NA)
Cai et al. (2016)	Case study	N95 filtering facepiece	1 patient (1)	NS (NS)
Worsley et al. (2016)	Comparative study	NIV-mask	13 patients (6)	25 (21-32)
Kant et al. (2017)	Cohort study	Transparent polycarbonate facial mask with silicone sheeting	21 patients (9)	57 (34-80)
Alqahtani et al. (2018)	Cohort study	Oronasal mask	15 patients (10)	26 (24-28)
Colla et al. (2019)	Technical note	Transparent face mask with silicone lining	1 patient (NS)	NS (NS)
Melia et al. (2019)	RCT	Force controlled algometer	100 volunteers (57)	NS (18-66)
Pilley et al. (2011)	Case study	Face mask	1 patient (0)	9 (NA)
Wei et al. (2017)	Case series	Face mask	2 patients (2)	3.5 (1-6)
Cai et al. (2018)	Case series	N95 FFR face seal	3 volunteers (NS)	NS (NS)
Shikama et al. (2018)	RCT	Fitting device for NIV oronasal mask	20 volunteers (3)	NS (NS)
Wei et al. (2018)	Pilot study	Face mask	10 patients (7)	31.5 (14-50)
Ozi et al. (2019)	Feasibility study	Facial padding	1 patient (1)	NS (NS)
Guilar et al. (2019)	Case study	Face mask for securing dermal substitutes and skin grafts and pressure therapy	1 patient (1)	38 (NA)

Abbreviations: NA - not applicable; NS - not specified

Table 3 Specifications of 3D scanning, CAD and 3D printing techniques and materials

Authors (year of publication)	Scan technique	Portability	Computer aided design (CAD)	Print technique	3D-printed material(s)	Transparency / Biocompatibility	Biocompatible silicones
De Crescenzo et al. (2011)	Laser-beam technology (NextEngine Desktop 3D Scanner, NextEngine Inc.)	Static	Mirroring and superimposing (Rapidform CAD, Version 2006 INUS Technology Inc. and Rhinoceros 4.0)	Fused deposition modeling (Stratasys)	ABS P400	Yes / Yes	Yes
Briggs et al. (2016)	Laser beam technology	NS	Editing to create a personalized mask (free opensource 3D application Blender)	Fused deposition modeling (Ultimaker 2, Ultimaker)	NS	No / Yes	No
Goyanes et al. (2016)	Structured light technology (Sense 3D, 3D systems Inc.)	Hand-held	Design (Meshmixer v.10.9.332, Autodesk Inc., USA)	(1) Fused deposition modeling (MakerBot Replicator 2X, MakerBot Inc., USA) and (2) Stereolithography apparatus (Form 1+ Stereolithography 3D printer, Formlabs, UK)	(1) NF (NinjaFlex) / Flex EcoPLA (FPLA) (iMakr, UK); (2) Polycaprolactone (PCL) / PEGDA, PEG and diphenyl(2,4,6-trimethylbenzoyl)phosphine oxide (Sigma Aldrich, UK);	NS / No	NA
Ayyildiz et al. (2018)	Photogrammetry (3dMDFace, Atlanta)	Static	Design (3-matic, Materialise)	Stereolithography apparatus (Formlabs, Form 2)	Semi-elastic durable acrylic resin	NS / No	NA
Bockey et al. (2018)	Photogrammetry (system developed by Bischoff et al.)	Static	NURBS curve to fit the virtual prosthesis to the facial surface (Rhinoceros, version 4.0, Robert McNeel & Associates)	Material jetting (OBJET EDEN 260V, Stratasys Ltd)	VeroDent MED-670, VeroDent Plus MED-690	NS / No	NA
Dipasquale et al. (2018)	Laser-beam technology (HandySCAN 300, Creaform)	Hand-Held	Cleaning and designing (Vxelements)	Fused deposition modeling (Ultimaker 3 Extended, Ultimaker)	PLA	NS / No	NA
Fan et al. (2018)	Structured light scanning and photogrammetry (Ipad and structure scanner)	Hand-held	Device design: prosthesis modelled on the facial contour	Material jetting (Objet500 Connex3, Stratasys Ltd)	NS	Yes / Yes	Yes
Sharma et al. (2018)	Structured light scanner (Sense 3D, 3D systems Inc.)	Hand-held	Repair and crop (MeshMixer, Autodesk), g-code (Slic3r)	Fused deposition modeling (M2, MakerGear)	PLA	No / No	No
Unkovskiy et al. (2018)	Photogrammetry (pritiface; pritidenta GmbH) and structured light technology (Artec Spider; Artec 3D)	Hand-held	Free-form sculpting (Zbrush software; Pixologic Inc.)	Material jetting (Drop-on-Demand ACEO, Wacker Chemie)	Silicone (ACEO Silicone General Purpose; Wacker Chemie AG)	No / No	No

Cevik et al. (2019)	Structured light technology (Artec Spider, Artec 3D)	Hand-held	NS (Artec 3D)	Fused deposition modeling (Makerbot Replicator 2)	PLA	No / Yes	Yes
LeCompte et al. (2019)	Structured light technology (iPhone X true depth cameras, scandly app)	Hand-held	Smoothing, aligning, boolean operation for subtraction (Geomagic Studio, 3D Systems)	Fused deposition modeling (MakerBot Replicator)	PLA (1.75 mm)	NS / NS	No
Makowski et al. (2019)	Structured light technology (Eva Artec, Artec 3D)	Hand-held	Cleaning and smoothing (Artec Studio 9 software)	Selective Laser Sintering (EOS Formiga P100)	Thermoplastic polyurethane (TPU) type 921A-1	NS / NS	No
Pilley et al. (2011)		Static	Aligning, cleaning (3-Matic, Materialise)	Binder jetting (Z510 Additive Manufacturing machining)	Aqueous binder printed on a bed of plaster	NA / NA	No
Wei et al. (2017)	Structured light technology (CREAFORM 3D, Go!Scan50)	Hand-held	Synthesizing several scans, indentation, releasing, smoothing, polishing (3-Matic, Materialise)	Material jetting (Objet, Stratasys Ltd.)	PolyJet material (OBJET MED610, Stratasys Ltd.)	Yes / Yes	Yes
Cai et al. (2018)	Laser beam technology (zgHandscan H100 scanner, Zhongguan Automation)	Hand-held	Reverse engineering, repair, NURBS (Geomagic Studio v.12.0, 3D system), design (Solidworks, Dassault Systèmes)	Fused deposition modeling (Allct FDM machine, Allcct Technology)	ABS	No / Yes	NA
Shikama et al. (2018)	Structured light technology (Eva 3D, Artec 3D)	Hand-held	Design mask (Artec Studio 10, Artec3D); Transformation to solid models (Geomagic Sculpt 3D software, 3D Systems)	Fused deposition modeling (Replicator 2X, MakerBot Industries)	NS	NS / NS	Yes
Wei et al. (2018)	Structured light technology (CREAFORM 3D, Go!Scan50)	Hand-held	Synthesizing several scans, indentation, releasing, smoothing, polishing (3-Matic, Materialise)	Material jetting (Objet, Stratasys Ltd.)	PolyJet material (OBJET MED610, Stratasys Ltd.)	Yes / Yes	Yes
Ozi et al. (2019)	Structured light technology (Sense, Cubify)	Hand-held	Repair (Geomagic Studio); Design padding (CATIA V5)	Fused deposition modeling (Flashforge Creator Pro)	PLA	No / Yes	Yes
Guilar et al. (2019)	Photogrammetry (3D scanner Crisalix)	Hand-held	Design mask (Crisalix Virtual Aesthetics, Crisalix)	Fused deposition modeling (Ultimaker 3 Extended, Ultimaker)	White PLA	No / Yes	NS

Table 4 Specifications of facial pressure (distribution) assessment tools

Authors (year of publication)	Outcome measures (unit)	Assessment tools	Location of measurement	Norm
Cheng et al. (1984)	Average pressure and range of pressure over different body parts (mmHg)	Sensors utilizing electro-pneumatic principles. Pressure is read off from a special Air-flow Measuring Manometer	Garment-scar interface (chin, cheek, malar region, forehead/neck, neck) and different part of the body in regions of different geometry	Above 25 mmHg. If the pressure can be maintained more constant at or above an 'optimal' level, one should be able to achieve better clinical results
Powell et al. (1985)	Interface pressure (NS)	(Absence of) appropriate blanching of the skin	NS	NS
Groce et al. (1999)	Interface pressure (mmHg)	Tek-scan and Mat-scan pressure measurement system.	Forehead, left and right cheek and the chin regions.	NS
Allely et al. (2008)	Skin perfusion (mean perfusion units – PU)	Laser Doppler imager LDI2 and software (Moor Instruments)	Entire facial area	NS
Van-Buendia et al. (2010)	Skin perfusion (mean perfusion units – PU)	Laser Doppler imager LDI2 and software (Moor Instruments)	Forehead, nose, chin, right cheek, left cheek	NS
Niezgoda et al. (2013)	(1) Z-forces (Pa) and (2) face seal area (cm <sup>2</sup> ) are utilized to determine the pressure distribution (Pa/cm <sup>2</sup> )	(1) Tensometer (Instron, Norwood, Mass.); (2) Stereophotogrammetry (3dMD and IMInspect, Polyworks software);	Face seal area	NS
Parry et al. (2013)	Mapping of areas of relief and compression (NS)	Polhemus laser scanner (Burlington) and FastScan software.	Entire facial area	NS
Cai et al. (2016)	Interface pressure (Pa) and resultant displacement (mm)	Finite element meshing of the headform and respirator CAD models (Hypermesh v12.0, Altair HyperWorks and LS-PREPOST en LS-DYNA, LSTC)	Nasal bridge, upper cheek, middle cheek, lower cheek, chin	NS
Worsley et al. (2016)	(1) Interface pressure (mmHg); (2) Temperature (°C) and humidity (% RH); (3) Comfort (VAS/10)	(1) Pressure monitoring system (Mk III, Talley Medical); (2) Sensirion SHT75 Sensor (Stafa, Sensirion AG); (3) 10-point VAS	Bridge of the nose and the superomedial aspect of left and right cheeks	NS
Kant et al. (2017)	Interface pressure (NS)	Aerial pressure sensor and pump	NS	Target pressure was 20 mmHg
Alqahtani et al. (2018)	(1) Interface pressure (mmHg); (2) Comfort (VAS/10)	(1) Oxford pressure monitor (18 mm sensor pads, Talley Group, Romsey, UK); (2) 10-point VAS	Nose bridge, left and right cheek	NS
Colla et al. (2019)	Interface pressure (mmHg)	Visually checking for blanching and Kikuhime pressure sensor	NS	Target pressure was 20 mmHg
Melia et al. (2019)	Peak pressure (N/cm <sup>2</sup> )	Ultra-thin (0.1 mm thick) tactile pressure sensor (Tekscan-I-scan System) used to assess pressure pain thresholds	Forehead, temple, chewing muscle	NS

Pilley et al. (2011)	Interface pressure (NS)	Visual assessment (based on experience)	Mask-scar interface	Between 24 and 30 mmHg
Wei et al. (2017)	Interface pressure (mmHg)	Observing blanching of scars through the transparent face mask and silicone gels reflect adequate pressure.	Mask-scar interface	At least 10-15 mmHg
Cai et al. (2018)	Interface pressure (Pa)	Pressure sensor (Arduino Uno R3 module, resistor kit, breadboard, jumper wires, slice type force sensitive resistor (Interlink Electronics Inc.)).	Nasal bridge, top of cheek, middle of cheek, bottom of cheek, chin	NS
Shikama et al. (2018)	(1) Strap tension (gf); (2) Interface pressure (mmHg); (3) Skin erythema (Erythema Index); (4) Comfort (10-point VAS)	(1) Stretchable strain sensor (Yamaha); (2) 12 thin (0.2 mm) sensors (FlexiForce, NITTA Corporation); (3) maximum Erythema Index calculated from digital images using ImageJ software; (4) 10-point VAS	Forehead, nasal bridge, left cheek, right cheek, chin	Less than 40 mmHg (the threshold of pressure ulcer formation)
Wei et al. (2018)	Interface pressure (mmHg)	(Thin and sensitive) PlianceX system (Germany-Novel Electronics, Munich); A finite element model of a head and an unmodified face mask was created to simulate and predict the mechanical response (ABAQUS FE package, Dassault Systems Simulia Corp., Providence, USA). Geometries were reconstructed from MRI (Philips AchieveNova 1.5T MR imager, Netherlands) in Mimics v14 (Materialize, Leuven, Belgium)	6 zones (forehead, eye, nose, mouth, cheek, chin)	Above 10 mmHg is acceptable in case of poor tolerance. Pressure is adjusted to the individual tolerance.
Ozi et al. (2019)	Interface pressure (mmHg)	A201 Flexiforce sensor (Tekscan, USA) with Arduino Uno microcontroller board for data acquisition	Forehead, nasal bridge, left cheek, right cheek	Less than 40 mmHg
Guilar et al. (2019)	Interface pressure (NS)	Interface pressure is optimized through the addition of a silicone lining	Mask-scar interface	NS

Abbreviations: NA - not applicable; NS - not specified